Forest Policy Report | SFI/2023

Remote Sensing Based Forest Inventory of Ukraine (RS-Inventory): Methodology, output maps, and estimates

Author:
Viktor Myroniuk

Contributors:
Axel Weinreich
Vincent von Dosky
Heino Polley
Matthias Dees

Kyiv, December 2023

About the Project “Sustainable Forestry Implementation” (SFI)

The project “Technical Support to Forest Policy Development and National Forest Inventory Implementation” (SFI) is a project established in the framework of the Bilateral Cooperation Program (BCP) of the Federal Ministry of Food and Agriculture of Germany (BMEL) with the Ministry of Environment and Natural Resources of Ukraine (MENR). It is a continuation of activities started in the forest sector within the German-Ukrainian Agriculture Policy Dialogue (APD) forestry component.

The Project is implemented based on an agreement between GFA Group, the general authorized executor of BMEL, and the State Forest Resources Agency of Ukraine (SFRA) since October 2021. On behalf of GFA Group, the executing agencies - Unique land use GmbH and IAK Agrar Consulting GmbH - are in charge of the implementation jointly with SFRA.

The project aims to support sustainable forest management planning in Ukraine and has a working focus on the results in the Forest Policy and National Forest Inventory.

Author:
Viktor Myroniuk

Contributors:
Axel Weinreich
Vincent von Dosky
Heino Polley
Matthias Dees

Disclaimer

This paper is published with assistance of SFI but under the solely responsibility of the author Viktor Myroniuk under the umbrella of the Sustainable Forestry Implementation (SFI). The whole content, particularly views, presented results, conclusions, suggestions or recommendations mentioned therein belong to the authors and do not necessarily coincide with SFI’s positions.

Contacts
Troitska Str. 22-24,
Irpin, Kyiv region
+38 (067) 964 77 02

TABLE OF CONTENTS

LIST OF ABBREVIATIONS

BA	Basal Area
CCDC	Continuous Change Detection and Classification
CNFI	Centre of National Forest Inventory
CI	Confidence Interval
FMP	Forest Management and Planning
FNF	Forest/non-forest
GEE	Google Earth Engine
GNN	Gradient Nearest neighbor
GREG	Generalized Regression
GSV	Growing Stock Volume
LB	Live Biomass
LC	Land Cover
LOO	Leave-One-Out
MAR	Model Assisted Regression
MSI	Multispectral Instrument
NBR	Normalized Burn Ratio
NDVI	Normalized Difference Vegetation Index
NFI	National Forest Inventory
OA	Overall Accuracy
OWV	Other Woody Vegetation
PA	Producer's Accuracy
RF	Random Forest
RS	Remote Sensing
SRTM	Shuttle Radar Topography Mission
TCT	Tasseled Cap Transformation
TPI	Topography Position Index
TS	Time Series
UA	User's Accuracy

SUMMARY

The National Forest Inventory (NFI) is the gold standard for assessing forest resources in support of the national forest policy. The implementation of the NFI methodology in Ukraine in its original form is violated by the ongoing Russian invasion which limits the collection of all necessary field data. In particular, large areas were not controlled by the Ukrainian government in 2023. It was also impossible to collect NFI data in many places close to the front lines or in areas contaminated by unexploded ordnance/land mines, radiation.

This situation can be overcome by technological advances in the combined use of field sampling data and remote sensing observations. Satellite imagery provides wall-to-wall coverage of large areas and additional information to support model approaches for retrieving forest information even in areas not visited during field campaigns. In line with these issues, a group of international and national short-term experts developed a Concept Study (Weinreich et al., 2023) for the implementation of the NFI over Ukraine using collected sample plot data, forest management and planning (FMP) information, in combination with satellite time series (RS-Inventory). This concept was then preliminary tested in the case study carried out in the Sumy region (Myroniuk, 2023) to elaborate technical details of data processing (sources of satellite data, processing platform, algorithms, etc.).

The concept of the RS-Inventory assumes the use of all available NFI data collected in 2021–2023 using a regular national-wide sampling design. For regions of Ukraine without NFI plots (Chernihiv, Kharkiv, Luhansk, Donetsk, Zaporizhzhia, Kherson, and AR of Crimea), forest stand characteristics were obtained from the most recent (less than 5 years) FMP data sets. The combining of both data sets, i.e., NFI and FMP data, and satellite observations provided the basis for implementing the RS-Inventory over Ukraine.

This report presents the description of the methodology, output maps, and estimates of the RS-Inventory within Ukraine. This is the first complex assessment of Ukraine's forests, which has been made possible by integrating expertise from different fields, including field sampling, statistical assessment, remote sensing, and modelling.

It is important to note that this study used the biophysical definition of forest as an area covered by woody vegetation with a predefined minimum canopy cover (>50%) observed at 20×20 m pixel level regardless of its legal status. Accordingly, the forest maps included categories (e.g. urban forests, cemeteries, etc.) that are not considered as forests according to Ukrainian regulations. Thus, the forest area according to the official definition can only be extracted using GIS overlay analysis within the boundaries of the State Forest Fund.

1. DATA SOURCES

The data used in this report came from a variety of sources. These included field data collection, remote sensing, and other supplementary geospatial information. Fixed area circular sample plots of the National Forest Inventory (NFI) and geospatial data collected in the Forest Management Planning (FMP) were two of the main sources of field observations. The need to include both data sources in this work was driven by the situation in Ukraine, where many areas are not accessible for safe field visits (temporarily occupied areas, areas along the front lines, contaminated areas, etc.). Time series (TS) of Sentinel 2 imagery were used for forest cover mapping and geospatial modeling of forest attributes. High-resolution Google Earth imagery was incorporated during the photointerpretation phase of the study. Other types of information included gridded layers of topographic features and climatic variables, boundaries of administrative oblasts (regions) of Ukraine, climatic ecozones, areas affected during the war.

1.1. Field observation data

1.1.1. NFI sample plots

The NFI sample plots in Ukraine were collected between 2020 and 2023 (Figure 1) using the nation-wide sample allocation design. This employs a random allocation of clusters of sample plots within a systematic reference grid of 5×5 km. Each cluster contains four fixed-area circular plots (500 m^2) arranged in the form of a square with 420 m spacing. During this period, about 3,000 sample plots were measured across Ukraine, but only 2634 forest sample plots were used in this project. Firstly, only sample plots that did not straddle different stands and were more than 75% forested were used (Figure 2). Second, plots were also excluded from the analysis if critical inconsistencies in forest attribute estimates were observed. For example, for some plots we found very low values (less than 0.3) of cylindrical form factors (Kershaw et al., 2016) derived from stand growing stock volume (GSV), basal area (BA), and height (HT).

Following the data structure proposed in the conceptual study, each sample plot was characterized by geographic coordinates of plot centers, a set of attributes related to administrative region, ecozone, forest type conditions, and site index. Measured (calculated) forest variables included mean age of the dominant tree species, mean diameter at breast height (DBH) of the dominant tree species and HT of the dominant tree species; total stand density (number of trees), BA and GSV; absolute and proportional estimates of BA for each species. These data were produced by the Centre of National Forest Inventory (CNFI) of Ukraine according to the requirements specified in the concept study (Weinreich et al., 2023).

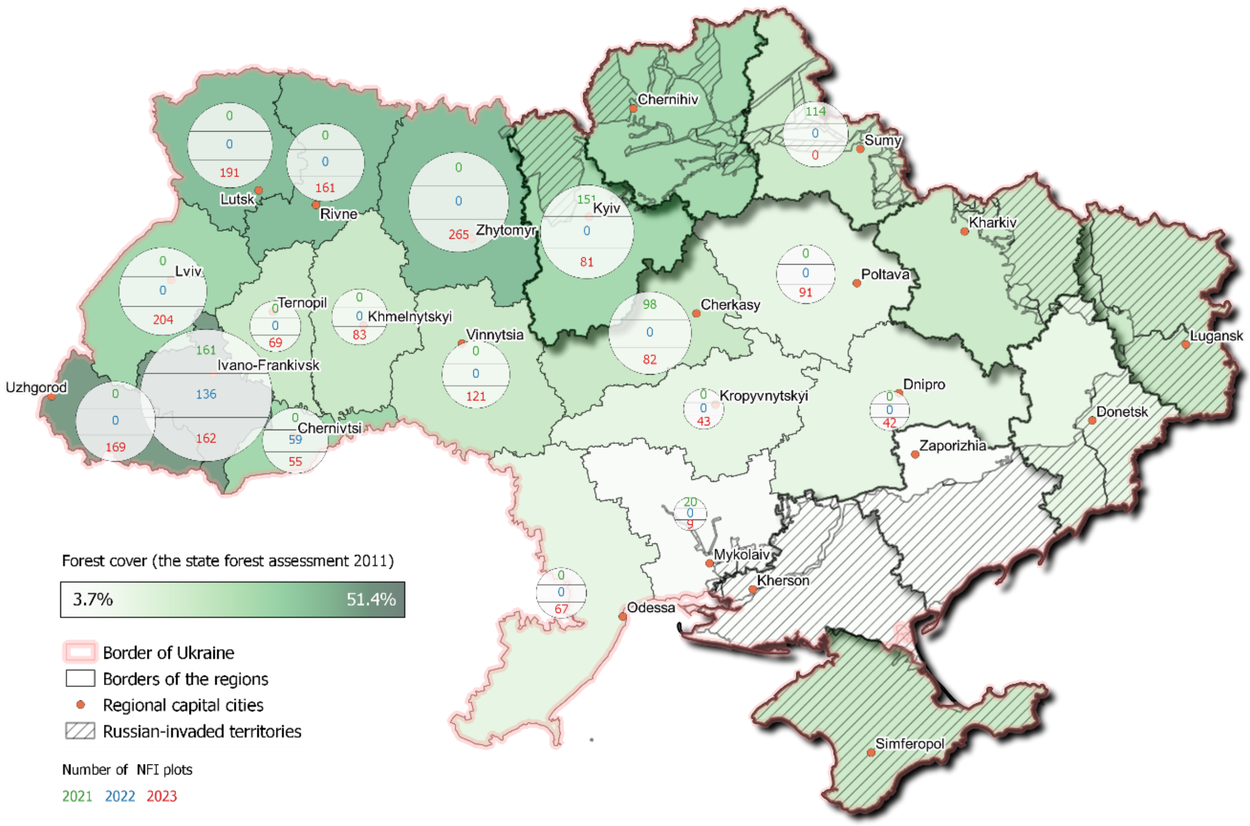

Figure 1. Distribution of the NFI sample plots used in the study.

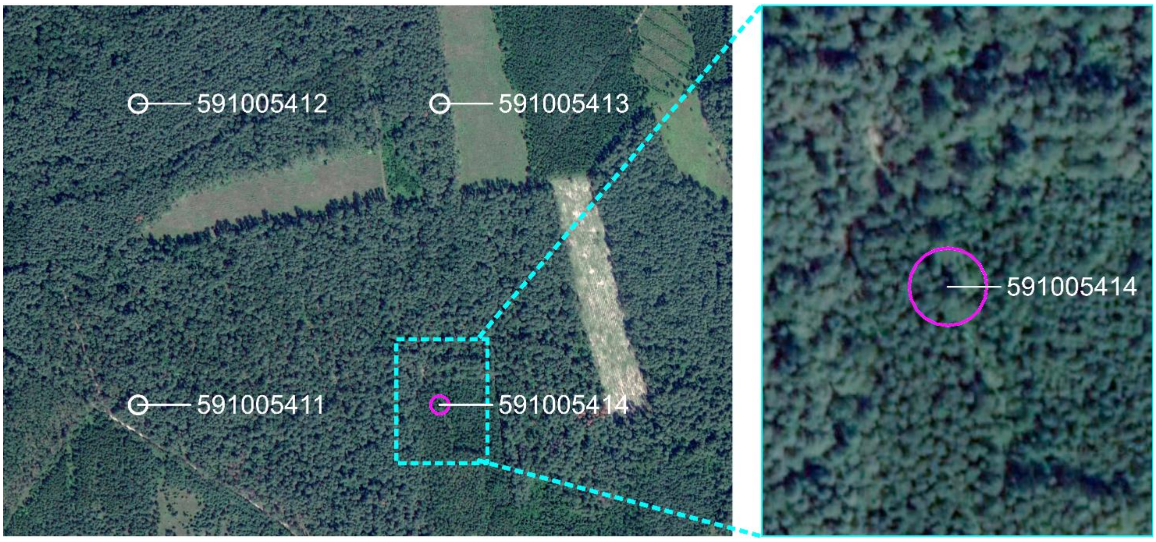

Figure 2. Example showing the issue when the plot (ID = 591005414) straddles different forest stands. Circles represent sample plots of 500 m² (plot radius is 12.62 m): white circles represent plots located within one forest stand; the magenta circle is a plot located within two different forest stands.

1.1.2. FMP training polygons

The most recent FMP data (between 2019 and 2021) were used only for regions where no NFI sample plots were collected, namely Chernihiv, Kharkiv, Luhansk, Donetsk, Zaporizhzhia, Kherson and AR of Crimea (see Figure 1). The FMP data included 1) a GIS coverage (ESRI shapefile) with boundaries of forest stands, and 2) a table (MS Excel spreadsheet) with selected forest attributes that can be used to obtain the same data structure as provided for the NFI plots. Note that the FMP collects average forest attributes observed within stands. Therefore, for large stands with non-uniform spatial structure, the information presented will not necessarily be correct in various parts of the stand. For example, stands may have different canopy closure, relative stocking, species distribution, etc. In addition, FMP estimates of age, mean HT, BDH and relative stocking were visually checked against material from the previous field survey, which was carried out about 10 years ago. Tree measurement tools (calipers, clinometers, relascopes) are mainly used in premature and mature stands via low-intensity sampling.

Reference samples were obtained from the FMP data in a series of steps.

1) We attempted to extract a balanced sample that approximated the one-phase (2023) sampling intensity of the NFI reference grid (Table 1). To do this, we extracted from the FMP data set all forest stands intersecting a 50-m buffer around NFI plots.

2) Trained interpreters visually analyzed the correspondence between FMP attributes of forest stands intersected by NFI plot centers and high-resolution Google Earth (GE) images (Figure 3).

3) These stands were used as potential candidates for delineating reference polygons only if the interpreters were satisfied with the provided information regarding relative stocking, species composition, age, HT, etc. Otherwise, another sampled stand was used as the candidate.

4) Within the candidate forest stands, training polygons were outlined to cover the most typical parts of the stands. We tried to use rectangular shapes (where possible) with an area of 0.1-0.8 ha.

Table 1. Distribution of FMP training polygons by region of Ukraine.

Region	Approximate number of planned NFI plots covered by forest according to official forest cover data	Number of training polygons collected using the FMP data
Chernihiv	213	243
Kharkiv	121	124
Luhansk	95	121
Donetsk	58	39
Zaporizhzhia	33	25
Kherson	36	41
AR of Crimea	91	109
Total	647	702

Unlike the NFI plots, which include estimates of species BA, the FMP data do not contain this information. Therefore, species BAs were calculated using yield tables for fully stocked forest stands (Bilous et al., 2020):

$$BA_{sp} = BA_{1.0} \cdot \frac{GSV_{sp}}{GSV_{1.0}},$$

where BA_{sp} – BA for given species, m^2·ha^{-1}; $BA_{1.0}$ – BA of fully-stocked (i.e., normal stand with relative stocking = 1.0) from yield tables, m^2·ha^{-1}; GSV_{sp} – GSV for given species from

FMP data, m³·ha⁻¹; $GSV_{1.0}$ – the relevant GSV of fully-stocked forest stand from yield tables, m³·ha⁻¹.

The yield tables use stand height as an input variable to obtain estimates of $BA_{1.0}$ and $GSV_{1.0}$ for given species. It is worth noting, that yield tables in Ukraine were compiled only for the main forest-forming species. BAs for other species were calculated using yield tables for corresponding substitute species (Table 2).

Stand densities (N_{sp}) were calculated using mean diameter for given species and estimated BA_{sp}:

$$N_{sp} = 40000 \cdot \frac{BA_{sp}}{\pi \cdot D_{sp}^2},$$

where D_{sp} – mean stand diameter for given species from the FMP data set, cm; π – 3.1416.

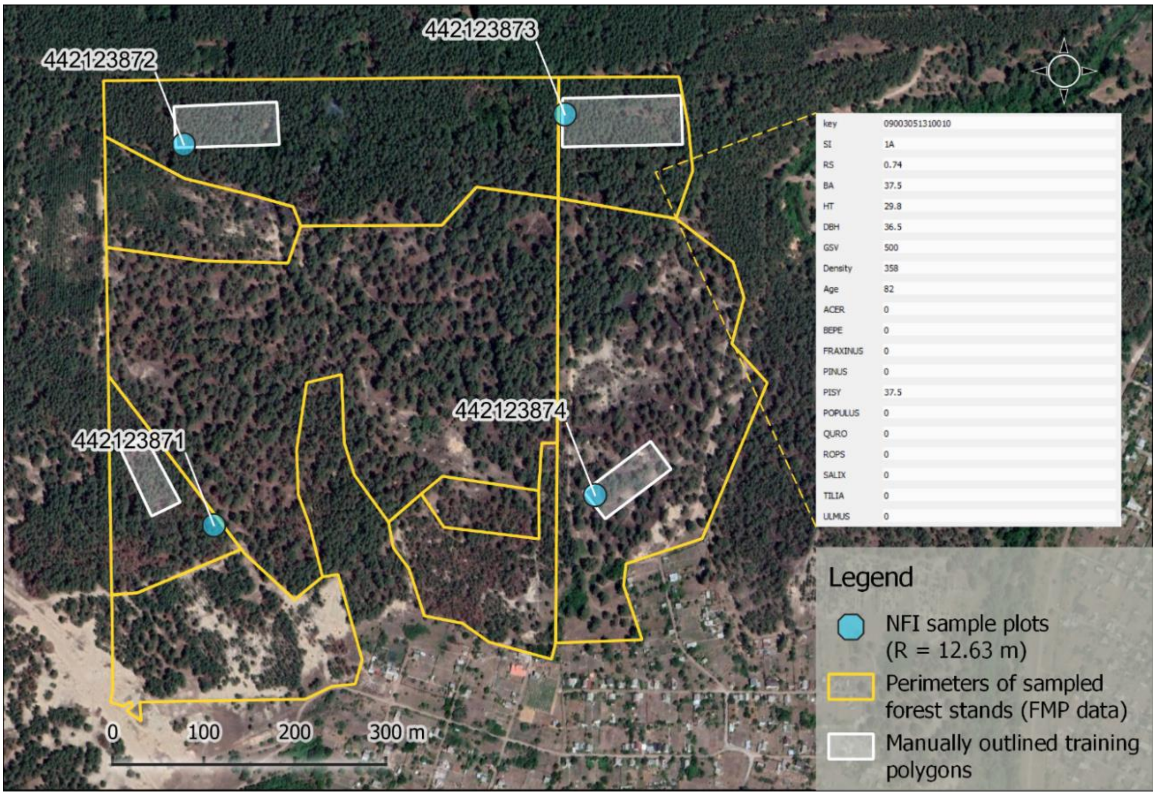

Figure 3. Example from the Luhansk region demonstrating the process of training polygons collection using FMP data in regions where NFI data could not be sampled. The attribute table represents the characteristics of the FMP stand updated during field surveys in 2021.

Once the required attributes had been calculated, the spreadsheets were linked to the shapefiles using a unique plot identifier (key field) in the following format – OOEEEDDBBBPPPS. The key field was constructed using the following stand attributes:

- OO – the code of the oblast (two digits, 59)
- EEE – the code of forest enterprise (three digits, e.g., 060)
- DD – the code of forest district (two digits, e.g., 01)
- BBB – forest block (three digits, e.g., 039)

- PPP – forest polygon (three digits, e.g., 020)
- S – forest sub-polygon (one digit, e.g., 0).

Table 2. Substitute species to estimate BA using yield tables.

Latin names	Genus	Substitute species
Abies alba	Abias	*Abies alba*
Acer campestre; A. hyrcanum; A. negundo; A. platanoides; A. saccharinum	Acer	*Carpinus betulus*
Acer pseudoplatanus	Acer	*Quercus robur (coppice)*
Aesculus hippocastanum	Aesculus	*Carpinus betulus*
Ailanthus altissima	Ailanthus	*Carpinus betulus*
Alnus glutinosa; A. incana	Alnus	*Alnus glutinosa*
Betula pendula; B. obscura; B. borysthenica	Betula	*Betula pendula*
Carpinus betulus; C. orientalis	Carpinus	*Carpinus betulus*
Celtis australis; C. occidentalis	Celtis	*Carpinus betulus*
Fagus sylvatica; F. orientalis	Fagus	*Fagus sylvatica*
Fraxinus americana; F. pennsylvanica; F. viridis	Fraxinus	*Quercus robur* (coppice)
Fraxinus excelsior	Fraxinus	*Quercus robur* (natural seed)
Gleditsia caspica; G. triacanthos	Gleditsia	*Robinia pseudoacacia*
Juglans ailantifolia; J. cinerea; J. mandshurica; J. nigra; J. regia	Juglands	*Quercus robur* (natural seed)
Larix decidua; L. sibirica	Larix	*Larix decidua*
Phellodendron amurense	Phellodendron	*Carpinus betulus*
Picea abies; P.orientalis; P. pungens	Picea	*Picea abies*
Pinus sylvestris; P. austriaca; P. banksiana; P. cembra; P. koraiensis; P. nigra; P. pallaciana; P. strobus	Pinus	*Pinus sylvestris*
Platanus occidentalis; P. orientalis	Platanus	*Carpinus betulus*
Populus tremula; P. alba; P. balsamifera; P. balsamilera; P. Bolleana; P. Canadensis; P. laurifolia; P. nigra; P. pyramidalis; P. suaveolens	Populus	*Populus tremula*
Prunus avium	Prunus	*Quercus robur* (natural seed)
Quercus robur (coppice); Q. Borealis; Q. petraea; Q; rubra; Q. pubescens	Querqus	*Quercus robur* (coppice)
Quercus robur (natural seed)	Querqus	*Quercus robur* (natural seed)
Quercus robur (planted seed)	Querqus	*Quercus robur* (planted seed)
Robinia pseudoacacia	Robinia	*Robinia pseudoacacia*
Salix alba; S. fragilis	Salix	*Salix alba*
Sophora japonicum	Sophora	*Robinia pseudoacacia*
Tilia cordata; T. platyphyllos	Tilia	*Quercus robur* (natural seed)
Ulmus laevis; U. glabra; U. minor; U. parviflora; U. scabra	Ulmus	*Carpinus betulus*

1.2. Sentinel 2 time series

This project utilized Sentinel 2 satellite TS acquired from March 26, 2017 to October 30, 2023. The TS represented surface reflectance images delivered as a Google Earth Engine (GEE) (Gorelick et al., 2017) collection – harmonized Sentinel 2 MSI, Level 2A. The collection was screened from clouds and cloud shadows using the Scene Classification (SCL) band classes. The following spectral data were used in the analysis: the original spectral bands; the first three primary components (brightness, greenness, and wetness) of the Tasseled-Cap Transformation (TCT) (Crist & Cicone, 1984), the Normalized Burn Ratio (NBR) (Key & Benson, 2006), and the Normalized Difference Vegetation Index (NDVI). Sentinel 2 images were resampled to 20-m spatial resolution.

1.3. Ancillary data

1.3.1. Ecoregions of Ukraine

We used the classification proposed by Gensiruk (1992), which distinguishes six main ecoregions in Ukraine (Fig. 4). These regions (forestry oblasts) are the largest unit in the Gensiruk's classification, described by common natural factors (climate and relief), forest characteristics, and principles of forest management. We used this classification in some stages of data analysis (i.e., assessing the accuracy of species classification) and reporting.

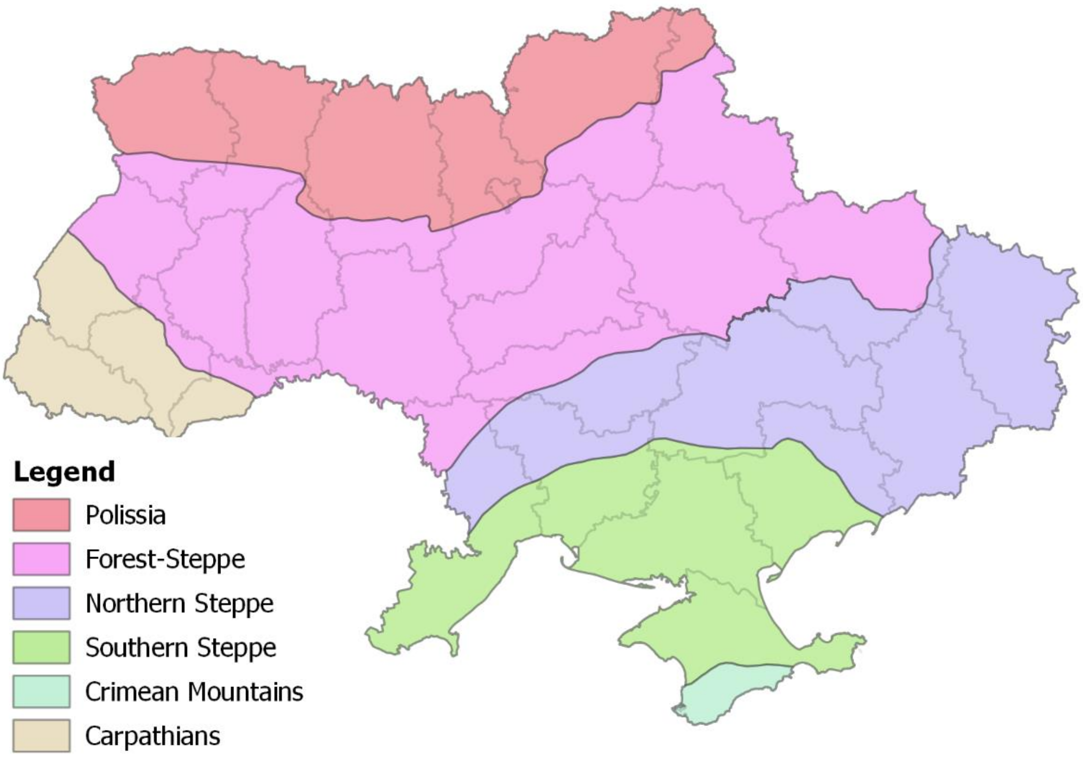

Figure 4. Ecoregions of Ukraine (forestry oblasts by Gensiruk (1992)) used in the RS-Inventory.

1.3.2. Environmental variables

The study also used additional environmental variables to improve the performance of the prediction models. These variables included elevation and topography position index (TPI)

(Weiss, 2001) extracted from the 90-m Shuttle Radar Topography Mission (SRTM), mean annual precipitation, and maximum July temperature (Abatzoglou et al., 2018).

1.4. Live biomass and carbon models

Live biomass (LB) and carbon stock were calculated using stand-level equations of conversion factors for the LB fractions (stems, branches, foliage, and roots), which are ratios of the corresponding biomass fractions to GSV (Shvidenko et al., 2014).

$$R_{fr} = \frac{M_{fr}}{GSV} = a_0 \cdot A^{a_1} \cdot SI^{a_2} \cdot exp(a_3 \cdot A), \quad (1)$$

$$R_{fr} = \frac{M_{fr}}{GSV} = a_0 \cdot A^{a_1} \cdot SI^{a_2}, \quad (2)$$

$$R_{fr} = \frac{M_{fr}}{GSV} = a_0 \cdot A^{a_1} \cdot SI^{a_2} \cdot RS^{a_3} \cdot exp(a_4 \cdot A + a_5 \cdot RS), \quad (3)$$

$$R_{fr} = \frac{M_{fr}}{GSV} = a_0 \cdot SI^{a_1} \cdot A^{(a_2 + a_3 \cdot RS + a_4 \cdot RS^2)}, \quad (4)$$

where R_{fr} is a ratio of LB fractions (M_{fr}) to growing stock volume (GSV); A is mean stand age, years; SI is site index (Table 3); RS is relative stand stocking.

The SI in eq. 1 and eq. 2 represents the top stand height at the age of 100 years. In contrast, the eq. 3 and eq. 4 use the integer codes of the SI classes.

Table 3. Site index classes of LB regression models (Shvidenko et al., 2014).

Equation	SI classification	Ukrainian SI classes by M. Orlov									
		Ia	Ib	Ia	I	II	III	IV	V	Va	Vb
1, 2	Top height (seed origin), m	43	39	35	31	27	23	19	15	11	7
1, 2	Top height (coppice origin), m	35.5	32.0	28.5	25.0	21.5	18.0	14.5	11.0	7.5	4.0
3, 4	Integer code	3	4	5	6	7	8	9	10	11	12

The stand-level LB models were developed only for seven major forest forming species in Ukraine (pine, spruce, oak, beech, birch, aspen, alder). Therefore, we also used substitute species in the LB calculations (Table 4). The carbon stock was estimated as LB times 0.47, and the CO_2-equialent was derived as LB×0.47×3.66667.

Table 4. Coefficients of the LB regression models (Shvidenko et al., 2014).

LB fraction	Equation	a_0	a_1	a_2	a_3	a_4	a_5
Pine: Pinus sp., Larix decidua							
Foliage	1	172.09	-1.602	-1.17	0.011		
Branches	1	110.23	-1.013	-1.272	0.007		
Stem	1	0.26	0.071	0.021	0.0026		
Root	1	4.96	-0.218	-1.08	0.0088		
Spruce: Picea sp., Abies alba							
Foliage	4	0.1008	0.4192	-0.117	-0.591	0.1585	
Branches	4	0.1124	0.4524	-0.0407	-0.837	0.4922	
Stem	4	0.1861	0.0814	0.1158	0.0811	-0.071	
Root	4	0.2845	0.3641	-0.332	0.2611	-0.413	
Oak: Querqus sp.; Acer sp., Carpinus sp., Fraxinus sp., Juglans sp., Ulmus sp.							
Foliage	1	43.202	-1.157	-1.062	0.002		
Branches	1	3.615	-0.143	-0.805	-0.0039		
Stem	1	0.377	-0.0446	0.144	0.002		
Root	1	0.000696	-1.131	2.643	0.015		
Beech: Beach sp.							
Foliage	1	547.4	-1.671	-1.391	0.012		
Branches	1	8.085	-1.277	-0.242	0.029		
Stem	1	0.251	0.199	0.086	-0.004		
Root	3	0.3696	-0.561	0.5132	-0.879	0.0054	0.356
Birch: Betula sp., Robinia pseudoacacia							
Foliage	2	1221.2	-0.826	-2.332			
Branches	2	202.21	-0.773	-1.464			
Stem	2	0.53	0.0277	-0.0226			
Root	2	1.206	-0.33	-0.272			
Aspen: Populus sp., Salix sp., Tilia sp.							
Foliage	2	57.749	-0.95	-1.557			
Branches	2	7.228	-0.339	-1.19			
Stem	2	0.896	-0.04	-0.214			
Root	3	1.0694	-0.3372	0.2435	0.7394	0.0007	-1.1848
Alder: Alder sp.							
Foliage	2	1.926	-0.75	-0.749			
Branches	2	0.129	-0.291	0.032			
Stem	1	0.185	0.243	0.084	-0.005		
Root	2	0.482	-0.02	-0.393			

2. Methods

2.1. Visual interpretation of the NFI data

All NFI sample plots for the one-year phase (2023) were visually interpreted from the GE imagery by a team of photo-interpreters working independently of the mapping team. The collected data were used for land cover (LC) classification and forest mask extraction. Visual interpretation was performed using the Collect Earth plugin (Bey et al., 2016) and a custom two-level classification scheme. This scheme included seven main LC classes, which in turn had several subclasses.

1. **Forest**
   1.1. Shelterbelt
   1.2. For. regrowth (CC>25%)
   1.3. Urban forest (parks)
   1.4. Other forest
2. **Other woody vegetation (OWV)**
   2.1. Forest edge
   2.2. Damaged forest
   2.3. Shrubland
   2.4. Orchard
   2.5. Garden trees
   2.6. OWV
3. **Grassland**
   3.1. Meadow
   3.2. Barren
   3.3. Glade
   3.4. Other grassland
4. **Cropland**
   4.1. Fallow cropland
   4.2. Irrigated cropland
   4.3. Other cropland
5. **Wetland**
   5.1. Season water
   5.2. Peatland
   5.3. Riparian vegetation
6. **Water**
   6.1. Permanent river
   6.2. Permanent lake
   6.3. Sea
7. **Urban (unproductive)**
   7.1. Highway
   7.2. Building
   7.3. Infrastructure
   7.4. Other urban area
   7.5. Other unproductive lands

Interpretation was carried out within squared photo-plots of 0.25 ha containing a regular grid of 5×5 control points. These points helped to identify the dominant LC if the plot straddled different LC categories. The interpreters followed the same rules in their interpretation:

1) The minimum LC area under the footprint of the photo-plot was greater than 0.25 ha.

2) The assigned LC class had occupied more than 50% of the photo-plot area, i.e., contained more than 13 control points.

3) The LC class showed no change within ±1 year of the image date used for interpretation.

4) The interpretation was carried out within a time window of May 2019 – August 2023.

5) Seasonal changes in LC variations have been considered for a more accurate interpretation.

6) Each photo-interpreted plot was assigned a confidence level (yes/no).

The atlas of sample images used in photo-interpretation (Table 5) is provided in the Annex A, while the Collect Earth plugin interface is shown in Figure 5.

Table 5. Distribution of sample plots between LC categories.

Administrative oblast	Forest	OWV	Grassland	Cropland	Wetland	Water	Urban (unproductive)	Total
Chernihiv	243	57	197	490	21	12	6	1026
Chernivtsi	68	31	32	101	11	1	6	250
Cherkasy	100	53	56	402	18	44	1	674
Dnipropetrovsk	43	28	148	737	12	40	22	1030
Donetsk	58	72	193	456	12	7	38	836
Ivano-Frankivsk	198	34	83	114	16	1	5	451
Kharkiv	167	65	110	605	36	16	22	1021
Kherson	24	14	68	626	13	100	47	892
Khmelnyntskyi	83	54	55	427	14	14	12	659
Kirovohrad	52	38	95	551	9	18	2	765
Kyiv	224	63	167	403	20	41	22	940
Lugansk	104	77	227	417	15	1	18	859
Volyn	271	35	107	218	11	7	8	657
Lviv	254	78	140	198	19	4	16	709
Mykolaiv	20	14	80	628	4	33	4	783
Odesa	66	29	145	744	33	61	18	1096
Poltava	102	47	119	592	23	40	3	926
Rivne	266	39	93	170	39	6	12	625
AR Crimea	105	28	230	415	10	47	29	864
Sumy	144	66	95	412	32	4	14	767
Ternopil	88	26	34	273	6	4	10	441
Zakarpattia	258	36	69	48	1	4	4	420
Vinnytsia	127	59	102	545	6	10	2	851
Zaporizhzhia	26	15	74	681	11	63	16	886
Zhytomyr	330	58	188	336	16	3	11	942
Total	3421	1116	2907	10589	408	581	348	19370

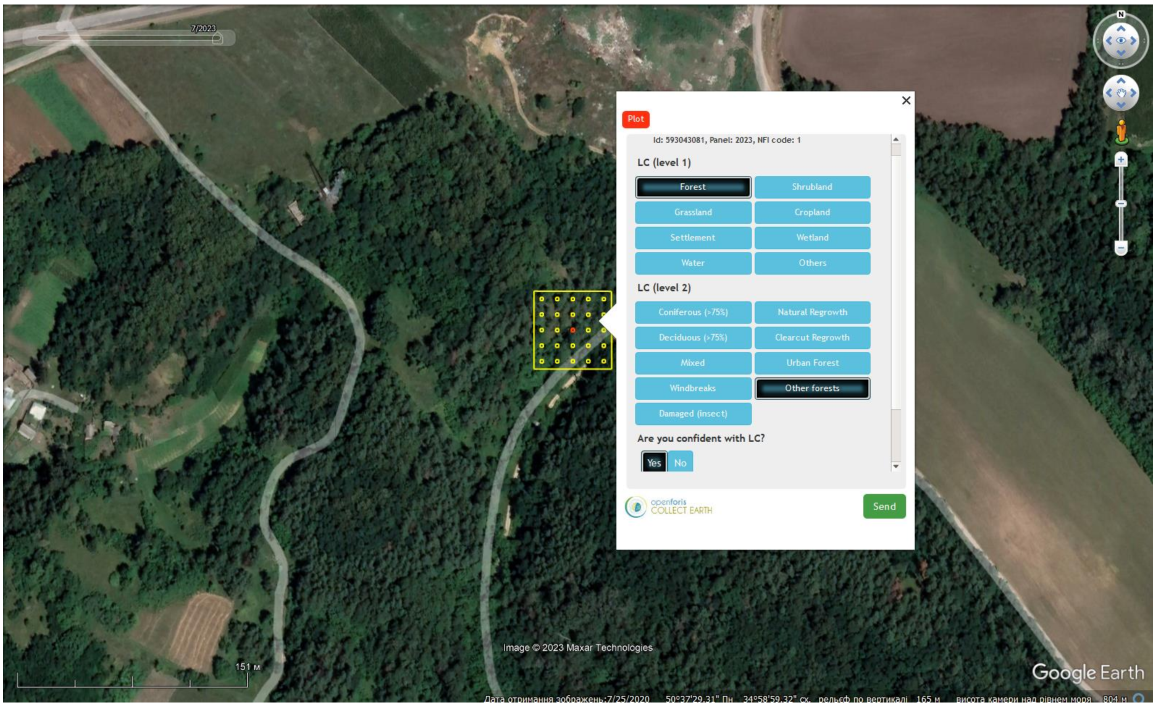

Figure 5. The Collect Earth plugin user interface.

2.2. Processing Sentinel 2 images

The data processing workflow used the high-performance GEE cloud-computing technology (Gorelick et al., 2017), which accelerated many steps of image processing. In addition, Quantum GIS and R software were used for data preparation, data analysis, and final maps production.

2.2.1. Temporal segmentation of satellite time series

Unlike many applications that use seasonal image mosaics (e.g., monthly or annual), this study used temporally smoothed Sentinel 2 TS. Temporal segmentation was performed using the Continuous Change Detection and Classification (CCDC) algorithm (Zhu & Woodcock, 2014). This approach is based on a harmonic regression, which captures cyclic patterns of spectral reflectance according to vegetation phenology throughout the year. The CCDC algorithm uses all available clear (from clouds, cloud shadows, and snow) pixel-level observations and divides the TS into consecutive segments corresponding to stable spectral trajectories without LC change. The harmonic model coefficients can be used to create a synthetic image for any date for which time series are available or used as a predictor variable in classification.

The image collections were segmented using all available spectral bands, three components of TCT, NBR, and NDVI. The CCDC algorithm used default settings regarding probability thresholds to change detection, a minimum number of observations to flag changes, etc. (Zhu & Woodcock, 2014).

Given the large volume of information, image processing was performed using a systematic 0.5×1-degree tiles seamlessly covering the territory of Ukraine (Figure 6). We used four WGS 84 / UTM zone 34-37N projections to store the processed tiles as GEE assets.

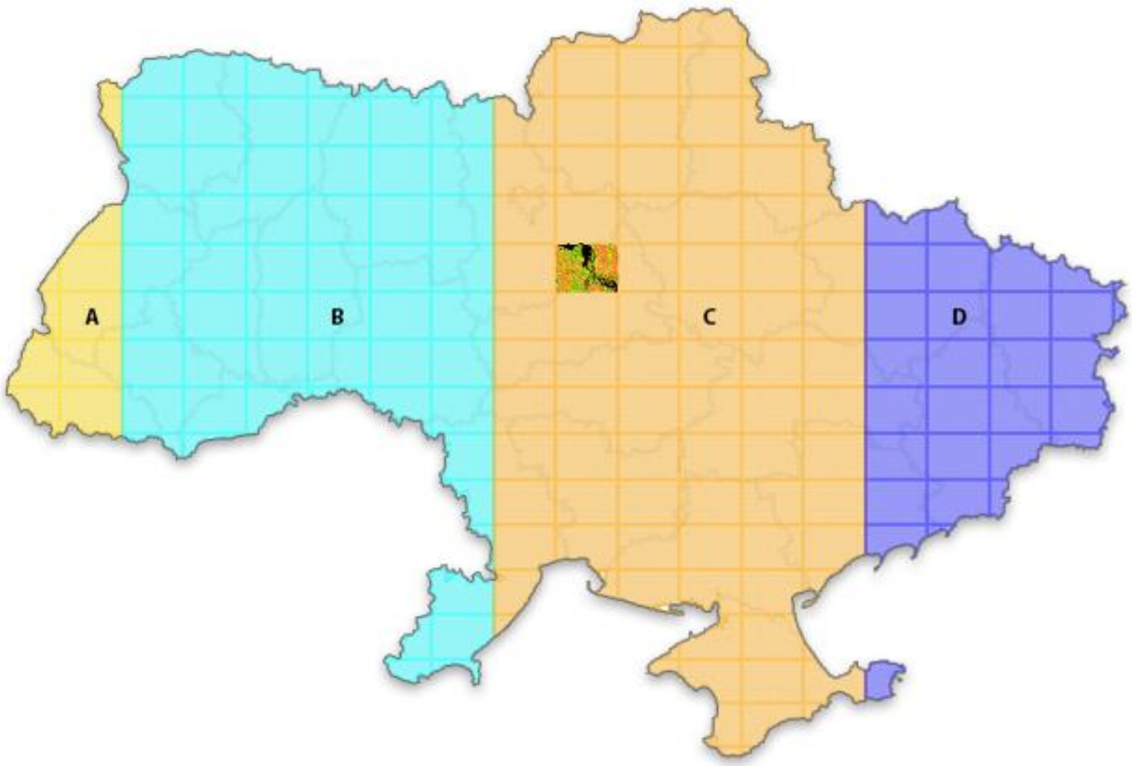

Figure 6. Regular 0.5×1-degree grid covering Ukraine with Sentinel 2 image tiles: (A) EPSG:32634; (B) EPSG:32635; (C) EPSG:32636; (D) EPSG:32637. The background uses the administrative boundaries of the regions of Ukraine.

2.2.2. Mapping forested area

The forested area was mapped using Random Forest (RF) classifier (Breiman, 2001). Similar to the previous study (Myroniuk, 2023; Myroniuk et al., 2022), only spectral variables were used in the classification, which included synthetic values of spectral bands (brightness, greenness, wetness components of the TCT, and NBR) predicted for the start (April 15), middle (June 15), and end (October 15) of a leaf-on period. These variables were supplemented with coefficients of the CDDC harmonic models and derivations (phase, amplitude, and density of observations per segment). Image interpretation dates for all NFI plots (see Table 5) were intersected with corresponding segments of the CCDC image. We trained a single RF classification model for Ukraine which was used to predict the LC for 2023. It was then reclassified into a binary raster to obtain a FNF map.

LC maps were exported to GEE image assets as individual 0.5×1-degree tiles using the corresponding UTM coordinate reference system.

2.2.3. Mapping dominant tree species

Dominant tree species were similarly mapped using a RF classifier. In addition to the spectral variables used for LC classification, we also used coordinates (longitude and latitude) and elevation, which can act as a proxy for a variety of ecological drivers of species composition. We defined dominant species as those that had the highest BA values in the sampled plots.

The NFI and FMP training data sets were used independently to construct two exclusive classification models for the regions where these data were collected. To attain a higher precision of the forest attributes estimates associated with given species, we used seven broader dominant species groups: 1) pine; 2) spruce and fir; 3) common oak; 4) beech; 5) deciduous species with high life expectancy (maple, ash, linden, etc.); 6) deciduous species with low life expectancy (birch, alder, poplar, willow); 7) hornbeam. We believe that more detailed classification can be obtained only by developing more local classification models that need a substantially larger training dataset.

Dominant species were mapped within the forest map of 2023. Given two classification models, the output maps were exported to GEE assets for individual administrative oblasts of Ukraine in the unprojected WGS 84 coordinate reference system.

2.2.4. Mapping forest attributes

Forest attributes were mapped using the Gradient Nearest Neighbor (GNN) imputation (Myroniuk et al., 2022; Ohmann & Gregory, 2002). This approach is a multivariate prediction technique that can characterize a plant community structure as a cohesive unit, i.e., simultaneously predict combinations of different forest variables. Given the two types of field observation data used in this work (i.e., NFI and FMP), we developed two individual GGN models for regions where NFI plots were sampled (see Figure 1) and for those where training polygons were created using FMP data (see Table 1).

The GNN models were built using spectral and ancillary variables. The spectral variables included only three TCT components predicted for the start (April 15), the middle (June 15), and the end (October 15) of the leaf-on season. The auxiliary variables included coordinates (longitude and latitude) and altitude. After considerations, we decided not to use climatic variables which have coarse spatial resolution and resulted in unrealistic gradients of mapped attributes for steep terrain in the Crimean Mountains. A similar situation was encountered with the topographic position index (TPI450).

As response variables in the GNN models, we used per hectare values of total BA combined with BAs for individual species. Given the low occurrence of many rare species in the sampled data, we only used BA estimates for such individual species as *Pinus sylvestris, Picea abies, Abies alba, Querqus robur, Fagus sylvatica, Carpinus betulus, Robinia pseudoacacia, Acer pseudoplatanus.* BA for all other species were combined into genus groups.

2.3. Map accuracy assessment

We reported map accuracies at different spatial domains. At the highest level, we presented accuracies for the whole Ukraine. This included an accuracy assessment for the forest map and forest attributes. Then, we also calculated accuracies for maps of our tree species, groups of coniferous species and deciduous species. A similar procedure was used to assess the accuracy for Gensiruk's ecozones (Polissia; Forest-Steppe; Steppe and Crimean Mountains; Carpathian Mountains), war-affected and war-unaffected areas. The mask of such areas was extracted from the open sources (deepstatemap). We only calculated regional-level accuracies for the forest maps as we had enough observations for LC. For the maps with forest attributes, however, only pixel-based estimates were obtained.

In addition to the accuracy, we calculated the uncertainties of the estimates measured as 95% confidence intervals (CI).

2.3.1. Discrete LC and dominant species maps

The skills of the RF models (LC and dominant species) were assessed using k-fold cross-validation. In this procedure, reference datasets of observations are randomly divided into k groups or folds (we used k = 10 folds) of equal size. Each fold was recursively treated as a validation set, and the model was trained on the remaining k-1 folds. The trained models were then evaluated on the withdrawn fold not used in the training. The resulting lists of observed and predicted values were used to construct confusion matrices using the "good practices" protocol (Olofsson et al., 2014). The RF models were evaluated using 95% confidence intervals (CI) for estimates of producer's (PA), user's (UA), and overall (OA) accuracies.

Overall accuracy:

$$OA = \sum_{j=1}^{q} p_{ij}, \tag{5}$$

User's accuracy:

$$UA_i = {}^{p_{ij}}/_{p_{i\cdot}}, \tag{6}$$

Producer's accuracy:

$$PA_j = {}^{p_{ij}}/_{p_{\cdot j}}, \tag{7}$$

where p_{ij} is the proportion of area for the population that has map class i and reference class *j*; $p_{i}.$ is the row sum, i.e., proportion of area mapped as class i; $p._j$ is column sum, i.e., proportion of area of the class; q is number of classes.

2.3.2. Continuous maps of forest attributes

The accuracies of the GNN models were evaluated using seven independent nearest neighbors (Ohmann & Gregory, 2002). This is a modified leave-one-out procedure for assessing the accuracy of a nearest neighbor model. R^2 was used to report on the predictive performance of the models for continuous values of such mapped attributes such as BA, GSV, DBH, HT, age, density, LB, and carbon. We also plotted observed and predicted values along with 1 : 1 identity lines to show agreement between the data.

2.4. Estimation procedure

2.4.1. Map area estimates

In this project, we estimated 1) the total forested area, 2) the area of dominant species, and 3) the distribution of areas (1) and (2) by classes of stand age, DBH, HT, GSV, and intervals of terrain variables (altitude, slope). The estimates were provided for the whole

Ukraine, administrative regions, and ecoregions. Pixel areas obtained directly from maps may differ from the actual area due to confusion between mapped classes. Therefore, our estimates were accompanied by adjustment coefficients and standard errors (SE) derived from confusion matrices according to the "good practice" estimation procedure (Olofsson et al., 2014).

The direct estimator of the area proportion of a class k is simply the sum of the estimated area proportions obtained from the reference classification, i.e., the sum of column k of the confusion matrix (see Table 6).

$$\hat{p}_{\cdot k} = \sum\nolimits_{j=1}^{q} \hat{p}_{ik\cdot} = \sum\nolimits_{j=1}^{q} W_i \cdot \frac{n_{ik}}{n_{i\cdot}}, \tag{8}$$

where $\hat{p}_{ik\cdot}$ is W_i is the proportion of area mapped as class i; n_{ik} is the plot count of the class k in the ith mapped class; $n_{i\cdot}$ is the row total in terms of sample count for mapped class i; q is number of classes; j is reference class.

The standard error is estimated as follows:

$$S(\hat{p}_{\cdot k}) = \sqrt{\sum_{i=1}^{q} W_i^2 \frac{\frac{n_{ik}}{n_{i\cdot}} \cdot \left(1 - \frac{n_{ik}}{n_{i\cdot}}\right)}{n_{i\cdot} - 1}} = \sqrt{\sum_{i=1}^{q} \frac{W_i \cdot \hat{p}_{ik} - \hat{p}_{ik}^2}{n_{i\cdot} - 1}}. \tag{9}$$

The estimated area and the standard error of the estimated area are given by

$$\hat{A}_k = A \cdot \hat{p}_{\cdot k}, \tag{10}$$

$$S(\hat{A}_k) = A \cdot S(\hat{p}_{\cdot k}), \tag{11}$$

where A is the total map area.

An approximate 95% confidence interval is obtained as $\hat{A}_k \pm 1{,}96 \cdot S(\hat{A}_k)$.

It is important to note that this study used the biophysical definition of forest as an area covered by woody vegetation with a predefined minimum canopy cover (>50%) observed at 20×20 m pixel level regardless of its legal status. Accordingly, the forest maps included categories (e.g., urban forests, cemeteries, etc.) that are not considered as forests according to Ukrainian regulations. Thus, the forest area according to the official definition can only be extracted using GIS overlay analysis within the boundaries of the State Forest Fund.

2.4.2. Model-assisted estimation of forest attributes

The generalized regression (GREG) estimator represents a class of model-assisted estimators (MAR) that use auxiliary variables for all population units and an assisting model to calibrate the estimator. The GREG consists of the mean of the predicted values over the population and the model residuals (calculated from a sample). The estimation of the mean values of the forest attributes and the corresponding variances were based on the tutorial developed for forest inventory applications (McConville et al., 2020) and widely used in earlier studies (McRoberts et al., 2014, 2016). The calculation of the SE of the estimate as the square root of the variance were used to present the uncertainties.

GREG estimator:

$$\hat{\mu}_y = \frac{1}{n}\sum_{i\epsilon S}\left(y_i - \hat{m}(x_i)\right) + \frac{1}{N}\sum_{i\epsilon U}\hat{m}(x_i). \tag{12}$$

GREG variance:

$$\hat{V}(\hat{\mu}_y) = \left(1 - \frac{n}{N}\right)\frac{1}{n}\frac{1}{n-1}\sum_{i\epsilon S}\left(y_i - \hat{m}(x_i)\right)^2. \tag{13}$$

Confidence interval of model-assisted mean:

$$\hat{\mu}_y \pm t_{(n-1;1-\alpha/2)} \cdot \sqrt{\hat{V}(\hat{\mu}_y)}, \tag{14}$$

where N is the finite number of the population U units (pixels); n is the number of selected units (plots) for the sample S; y_i is the observed value for *i*-th unit; $\hat{m}(x_i)$ is the predicted value for the *i*-th unit given auxiliary data x; $t \approx 2$ for a 95% CI.

3. RESULTS

3.1. Forested area

The forested area was extracted from the corresponding LC map (Figure. 6). In this project, we report on two estimates of the forest area in Ukraine. The first one is the pixel area of the mapped class "forest". Since the classification model has different ability to classify LC types, the true forest area may differ from the pixel area. Therefore, we also used the second estimate of the forested area which was adjusted using information on the confusion between LC classes (Olofsson et al., 2014).

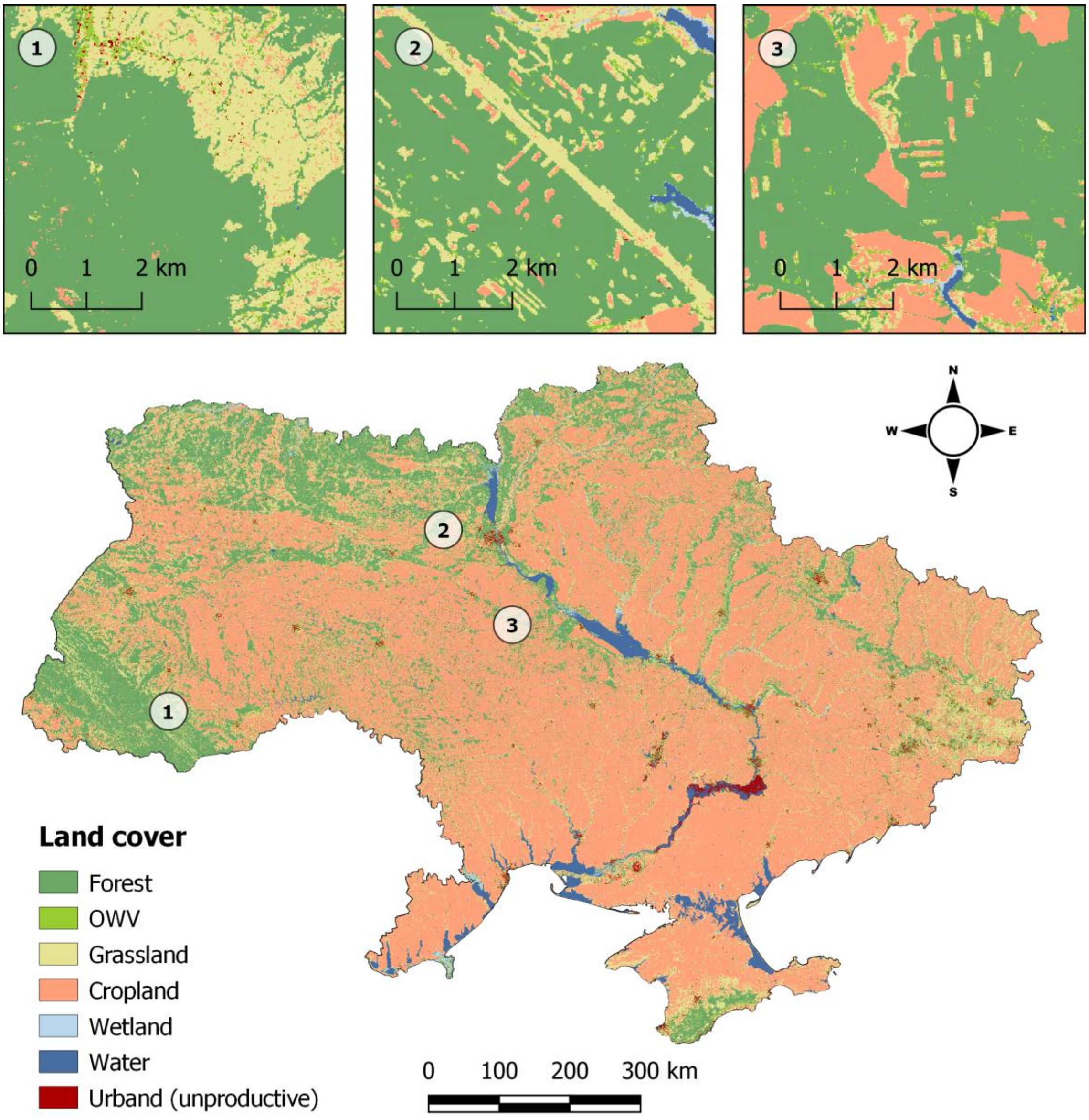

Figure 7. LC map of Ukraine (2023) derived from Sentinel 2 (20-m) TS. Close-up examples show different forest patterns within the Carpathian Mountains (1), Polissia (2), and Forest-Steppe (3).

The confusion matrix (Table 6) showed the errors of forest classification with OWV (garden trees, forest edges), grasslands (with scattered trees), and croplands (shelterbelts). The highly fragmented forest landscape in Ukraine is also one of the factors influencing forest misclassification. We used confusion matrices to adjust regional estimates of forested areas which we provided along with 95% confidence intervals of the estimates (Table 7).

Table 6. Confusion matrix of LC classification over Ukraine with cell entries expressed in terms of proportion of the total area (Olofsson et al., 2014) obtained.

Map	Reference								Mapped area, thousand ha
	Forest	OWV	Grass-land	Crop-land	Wet-land	Water	Urban	Total	
Forest	**0.172**	0.011	0.002	0.001	0.002	0.000	0.000	0.188	11335.4
OWV	0.007	**0.017**	0.005	0.002	0.001	0.000	0.002	0.033	1982.0
Grassland	0.004	0.013	**0.098**	0.018	0.005	0.000	0.003	0.14	8457.2
Cropland	0.004	0.004	0.027	**0.554**	0.002	0.001	0.002	0.593	35701.8
Wetland	0.000	0.000	0.001	0.000	**0.008**	0.000	0.000	0.01	573.9
Water	0.000	0.000	0.000	0.000	0.000	**0.026**	0.000	0.026	1587.1
Urban	0.000	0.002	0.001	0.000	0.000	0.000	**0.008**	0.01	593.7

Table 7. Regional accuracy of the FNF map of Ukraine for 2023.

Region of Ukraine	Forested area, thousands ha		Estimated area proportion	User's accuracy	Producer's accuracy	Overall accuracy of the LC map
	Mapped (pixel area)	Estimated*				
AR of Crimea	251.5	264.1±11.6	0.098±0.004	0.860±0.027	0.819±0.030	0.864±0.009
Vinnytsia	430.7	407.9±13.2	0.154±0.005	0.871±0.023	0.918±0.019	0.889±0.007
Volyn	816.4	801.8±15.3	0.398±0.008	0.945±0.014	0.962±0.012	0.870±0.013
Dnipropetrovsk	199.1	213.8±10.7	0.067±0.003	0.871±0.023	0.815±0.037	0.892±0.008
Donetsk	222.4	254.5±13.9	0.096±0.005	0.860±0.027	0.751±0.038	0.859±0.009
Zhytomyr	1141.9	1121.6±21.5	0.376±0.007	0.945±0.014	0.962±0.012	0.874±0.012
Zakarpattia	805.1	782.1±14.9	0.613±0.012	0.963±0.015	0.991±0.011	0.886±0.022
Zaporizhzhia	57.9	92.6±8.7	0.034±0.003	0.860±0.027	0.539±0.050	0.889±0.009
Ivano-Frankivsk	708.4	690.6±14.6	0.496±0.010	0.963±0.015	0.988±0.014	0.879±0.023
Kyiv	751.9	750.5±17.5	0.259±0.006	0.945±0.014	0.946±0.018	0.880±0.012
Kirovohrad	184.4	186.7±7.4	0.076±0.003	0.871±0.023	0.865±0.028	0.905±0.006
Luhansk	280.6	306.9±14.9	0.115±0.006	0.860±0.027	0.788±0.034	0.843±0.010
Lviv	848.6	833.8±21.7	0.382±0.010	0.963±0.015	0.981±0.021	0.862±0.026
Mykolaiv	60.5	73.1±5.1	0.030±0.002	0.871±0.023	0.724±0.049	0.910±0.006
Odesa	162.9	173.5±8.1	0.052±0.002	0.871±0.023	0.825±0.035	0.901±0.007
Poltava	322.5	313.1±11.1	0.109±0.004	0.871±0.023	0.893±0.023	0.892±0.007
Rivne	825.6	810.2±15.3	0.404±0.008	0.945±0.014	0.963±0.012	0.872±0.013
Sumy	573.4	529.2±15.4	0.222±0.006	0.871±0.023	0.944±0.013	0.876±0.009
Ternopil	251.8	233.8±6.9	0.169±0.005	0.871±0.023	0.938±0.014	0.894±0.007
Kharkiv	449.6	449.5±17.3	0.143±0.006	0.860±0.027	0.858±0.024	0.867±0.009
Kherson	54.4	82.1±7.5	0.030±0.003	0.860±0.027	0.576±0.053	0.897±0.008
Khmelnytskyi	364.6	344.4±10.9	0.167±0.005	0.871±0.023	0.922±0.018	0.886±0.008
Cherkasy	369.7	345.6±10.7	0.165±0.005	0.871±0.023	0.929±0.017	0.896±0.007
Chernivtsi	291.5	286.5±7.8	0.354±0.010	0.963±0.015	0.980±0.022	0.876±0.023
Chernihiv	910.2	845.0±27.0	0.265±0.008	0.860±0.027	0.928±0.013	0.858±0.011
Total	**11335.5**	**11203.0±166.1**	**0.186±0.003**	**0.911±0.010**	**0.922±0.010**	**0.881±0.005**

* The area estimates were adjusted according to the guidance by Olofsson et. al (2014).

3.2. Dominant tree species

Dominant species were mapped within forested areas using two RF classification models developed independently for regions of Ukraine using 1) NFI and 2) FMP data. We identified individual species (pine, spruce and fir, oak, beech, hornbeam) and species groups to attain higher accuracy in the classification (Figure 8). We believe that such classification provides a baseline for further improvement of the approach. Other species could be extracted from the identified species groups using local classification models. For example, we found more than 50 combinations of codominant species occurring in Ukrainian forests. Given the diversity of species composition, this issue deserves a more detailed investigation of the ecological niches that certain species might occupy. Otherwise, detailed species classification may lead to unacceptably high uncertainties in map-based estimates.

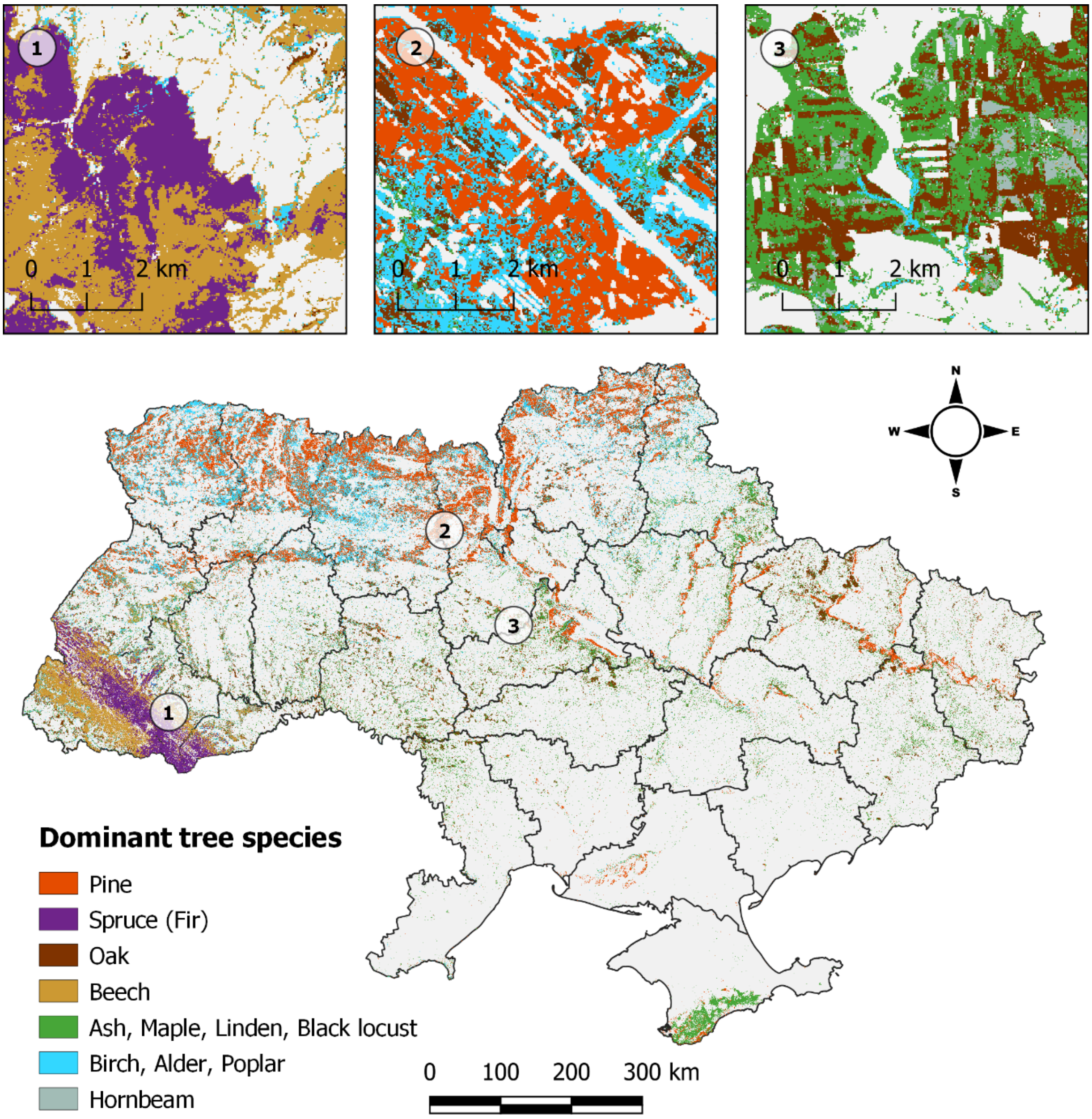

Figure 8. Map of dominant species (species groups) in Ukraine (2023) derived from Sentinel 2 (20-m) TS. Close-up examples showing the specific types of forest composition within the Carpathian Mountains (1), Polissia (2), and Forest-Steppe (3).

The accuracy of the classification was evaluated via confusion matrices. In addition to the mapped species, we also calculated the confusion between broader groups of coniferous and deciduous species. In the report, we present aggregated results for Ukraine (Table 8, Table 9). The overall accuracy of species classification was 0.763±0.015, and 0.945±0.008 for two major species groups.

Table 8. Accuracy of the dominant species map of Ukraine for 2023.

Species (species group)	Area, thousands ha		Estimated area proportion	User's accuracy	Producer's accuracy
	Pixel area	Estimated*			
Pine	3049.8	3139.9±92.6	0.277±0.008	0.918±0.018	0.890±0.021
Spruce (Fir)	718.6	736.8±43.6	0.065±0.004	0.886±0.035	0.867±0.043
Oak	1478.4	1666.3±114.2	0.147±0.010	0.663±0.041	0.590±0.037
Beech	951.8	782.1±60.8	0.069±0.005	0.702±0.051	0.854±0.041
Ash, Linden, Maple, Black locust	2406.8	2244.4±111.0	0.198±0.010	0.738±0.033	0.792±0.028
Birch, Alder, Poplar	2398.7	2244.6±133.2	0.198±0.012	0.671±0.043	0.716±0.030
Hornbeam	331.6	521.4±72.7	0.046±0.006	0.552±0.088	0.353±0.058

Table 9. Accuracy of dominant species group mapping within Ukraine for 2023.

Species group	Area, thousands ha		Estimated area proportion	User's accuracy	Producer's accuracy
	Pixel area	Estimated*			
Coniferous species	3768.4	3797.4±86.6	0.335±0.008	0.922±0.015	0.914±0.016
Deciduous species	7567.1	7538.1±86.6	0.665±0.008	0.957±0.009	0.961±0.007

* Area estimates have been adjusted according to the guidelines by Olofsson et. al (2014).

3.3. Continuous forest attributes

3.3.1. Basal area and growing stock volume

The maps of predicted BA and GSV are highly correlated, so we only provide an example for GSV in the report (Figure 9). The imputed maps have significant uncertainties at the 20-m pixel level. Therefore, for practical applications, we recommend using these data at a higher level of aggregation. For example, we found that even combining plot-level estimates into clusters can reduce (about 10%) the confusion between observed and predicted values (Figure 10).

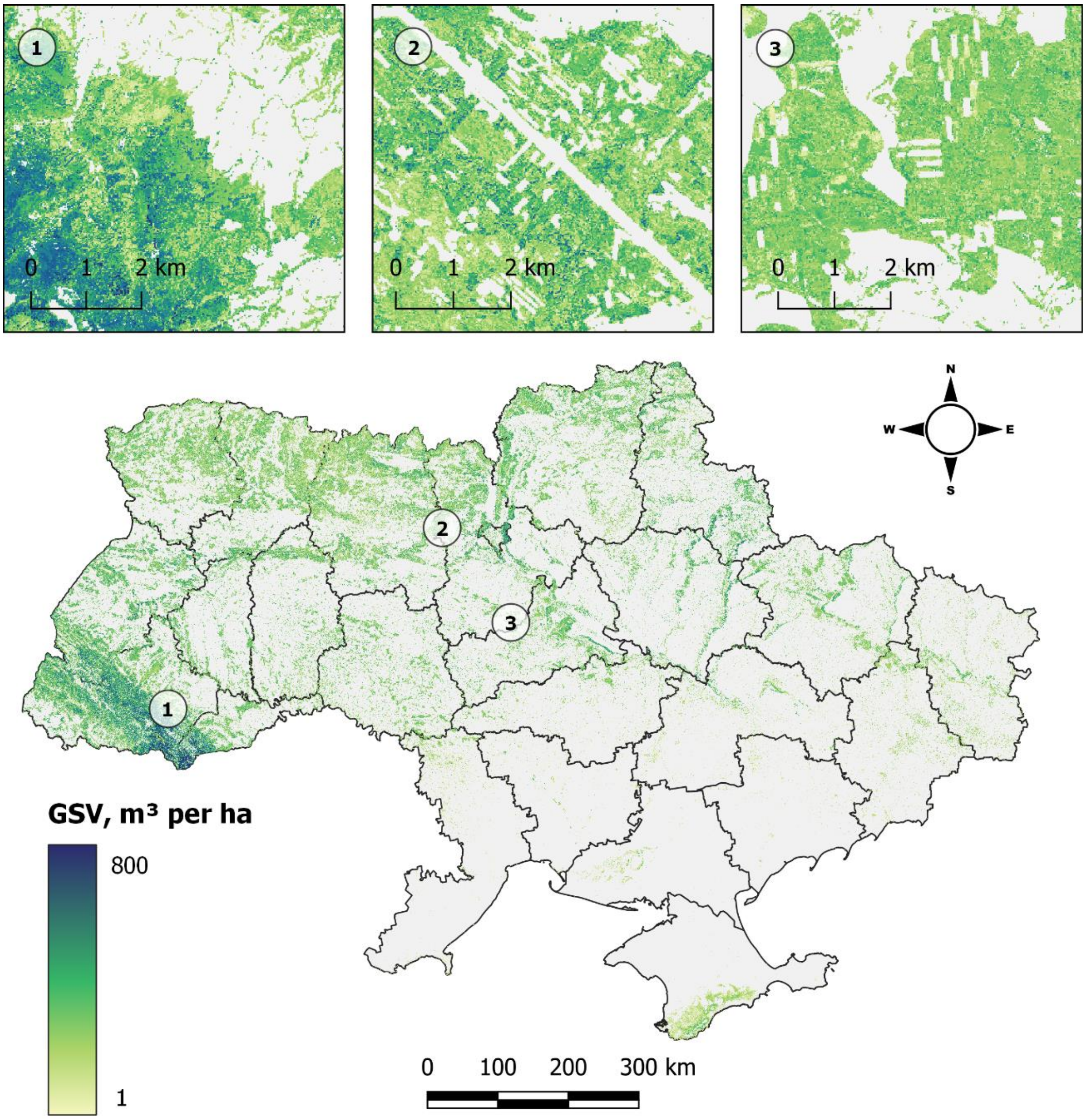

Figure 9. Mean GSV map of Ukraine (2023) predicted using Sentinel 2 (20-m) TS and GNN imputation.

Interestingly, the values of the coefficient of determination were higher for the GNN model developed using the FMP data (R^2 = 0.48-0.59) than for those using the NFI data (0.41-0.45). A possible explanation for this situation could be some issues with the correct GPS coordinates of the true NFI plot locations, which are relatively small areas (500 m^2). Any deviation from the original plot location in structurally diverse forests or in the case of forest edges could have a significant impact on the model performance. Therefore, it is critical for the future to ensure that all sampled plots have correct coordinate registration. This can be partially corrected visually using high resolution imagery.

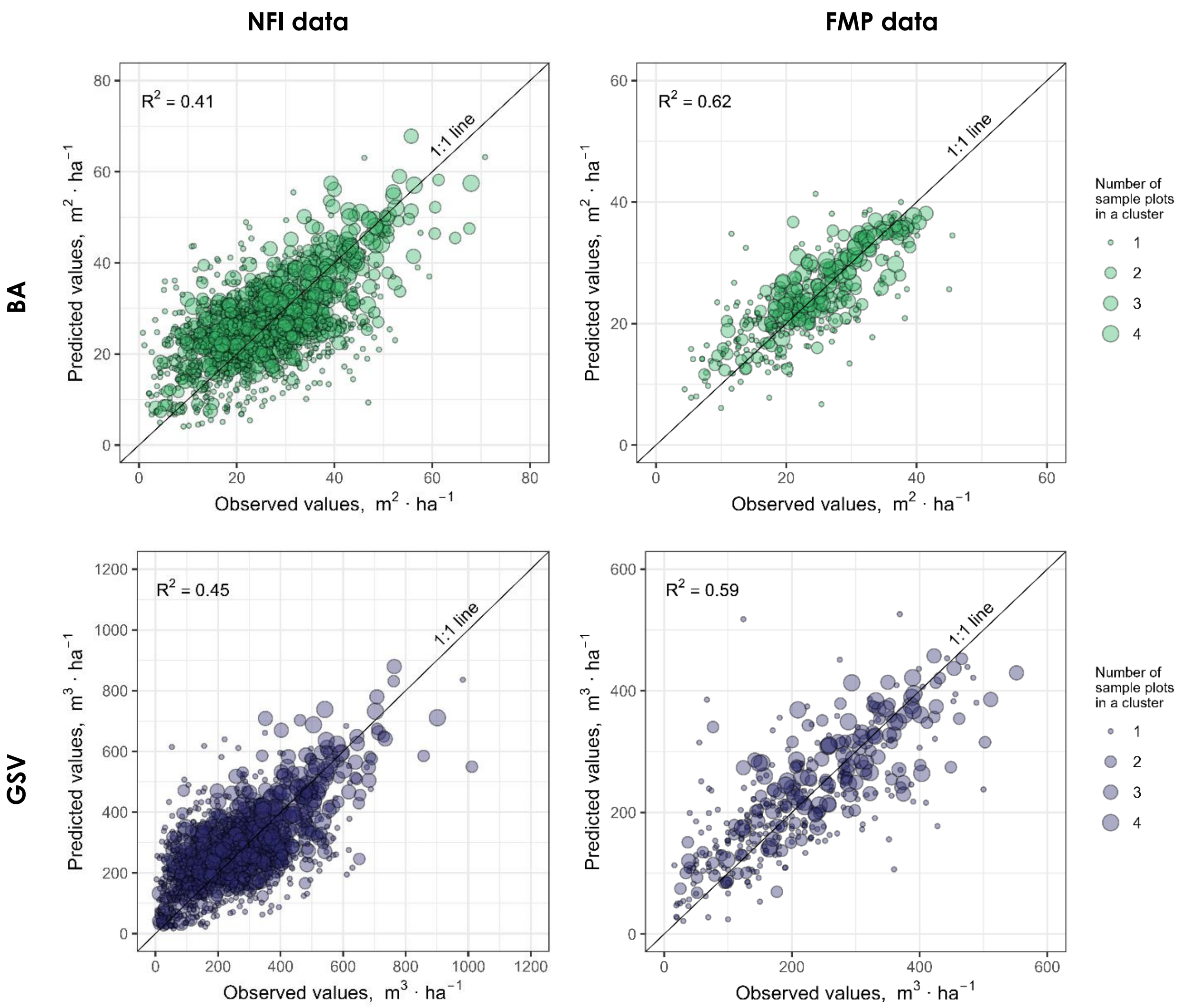

Figure 10. Observed versus predicted values of BA and GSV.

3.3.2. Mean age, DBH, HT, and carbon stock

All other forest attributes were imputed using the developed GNN model (Figure 11–14). An important advantage of the GNN multivariate prediction is that it treats each plot or pixel as a cohesive vegetation community unit with a specific combination of attributes. From this perspective, predicted combinations of forest attributes could potentially exist in nature (this is necessarily true if a GNN model with k =1 is used). All our predictions are characterized as medium, medium-low, and low coefficients of determination in a range of 0.15-0.6. Similar to BA, higher accuracy can be expected when pixel data are aggregated at stand level.

In this report, we have provided maps that have been directly imputed using the GNN models. However, maps for some other attributes (stand density, LB, CO_2-equialent) can be calculated from the presented maps. Regarding stand density, we found some limitations in predicting this attribute from optical remote sensing.

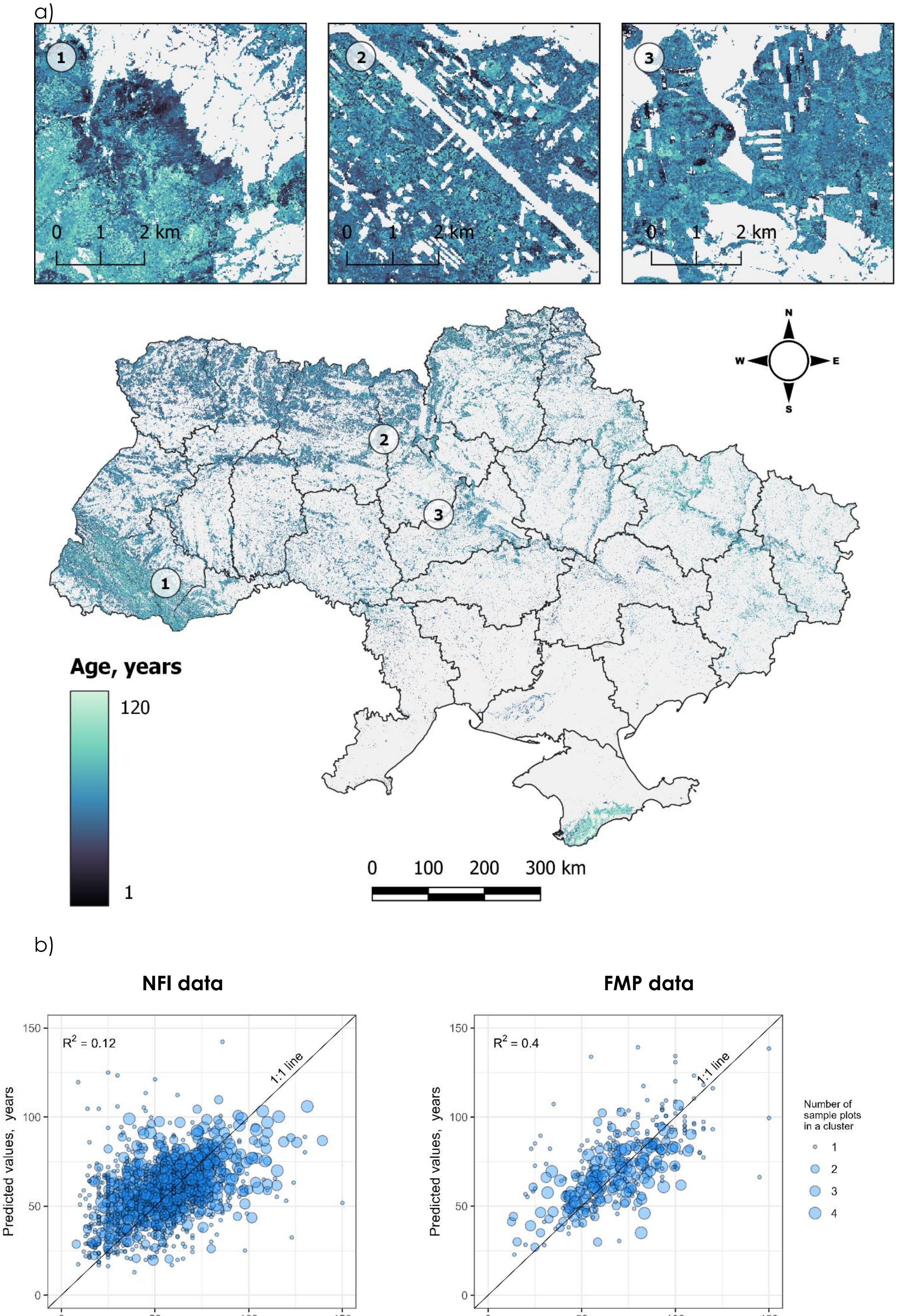

Figure 11. Mean stand age (2023): a) map predicted using the GNN imputation model, b) observed versus predicted values.

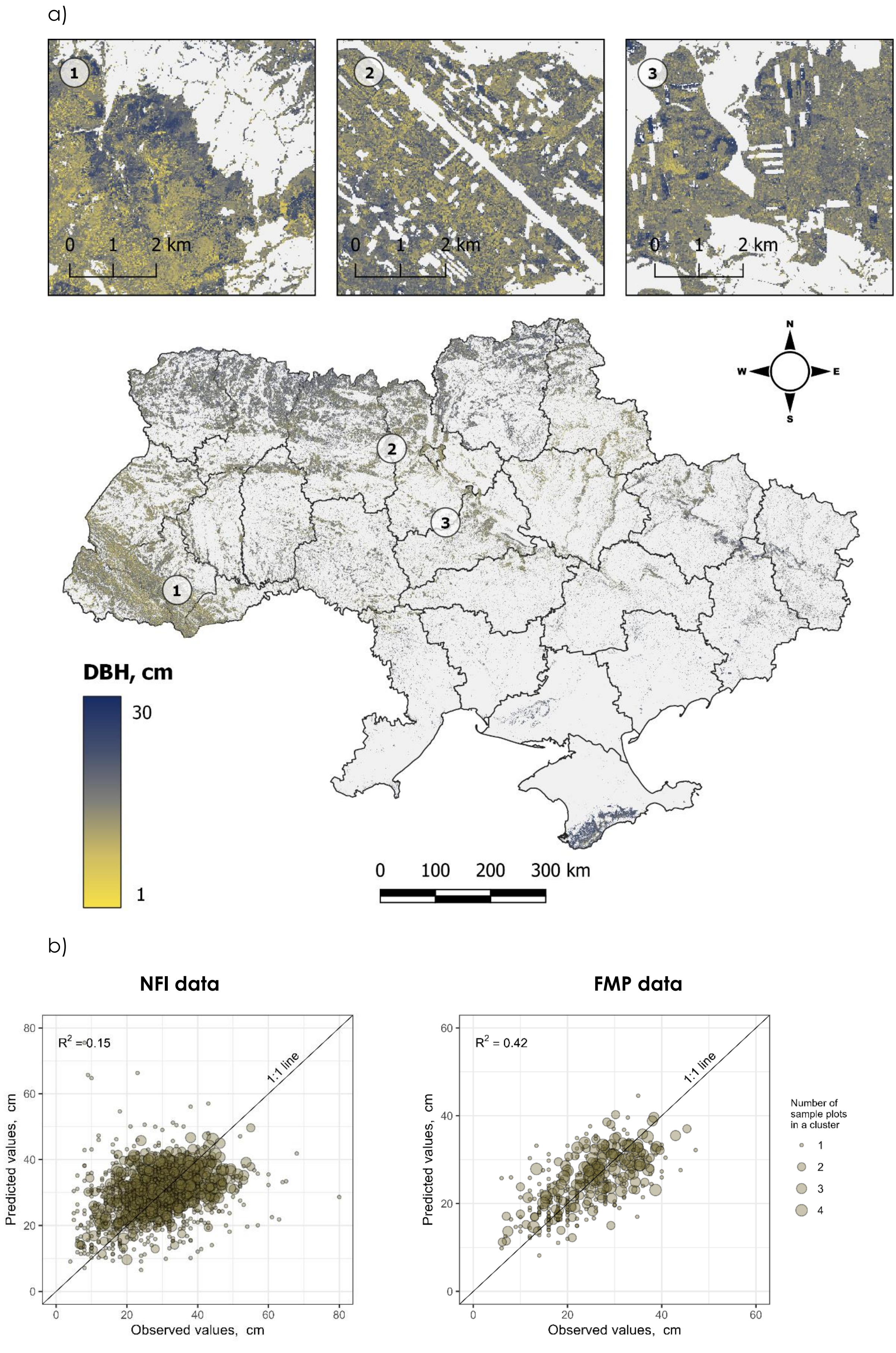

Figure 12. Mean DBH of forest stands (2023): a) map predicted using the GNN imputation model, b) observed versus predicted values.

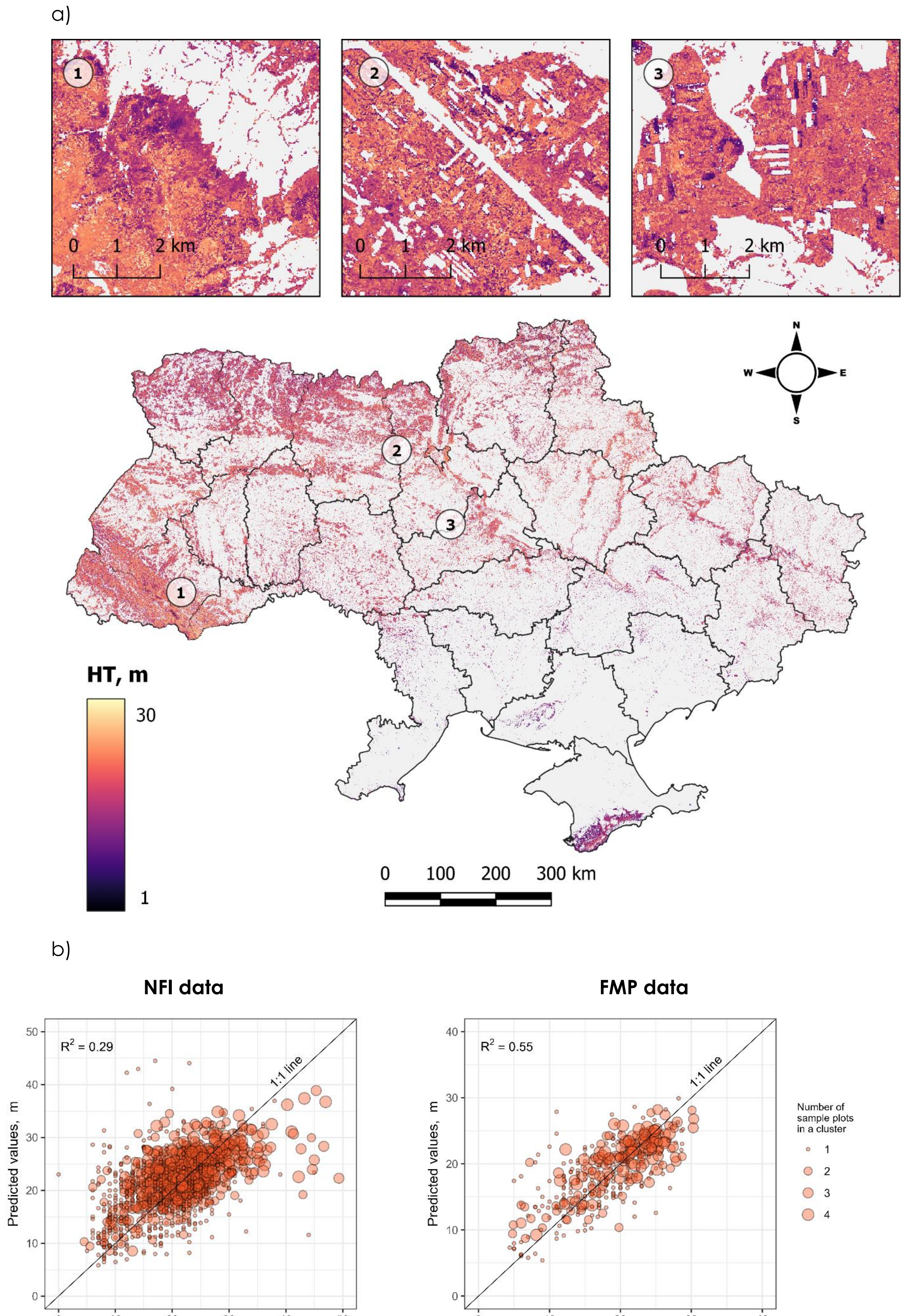

Figure 13. Mean HT of forest stands (2023): a) map predicted using the GNN imputation model, b) observed versus predicted values.

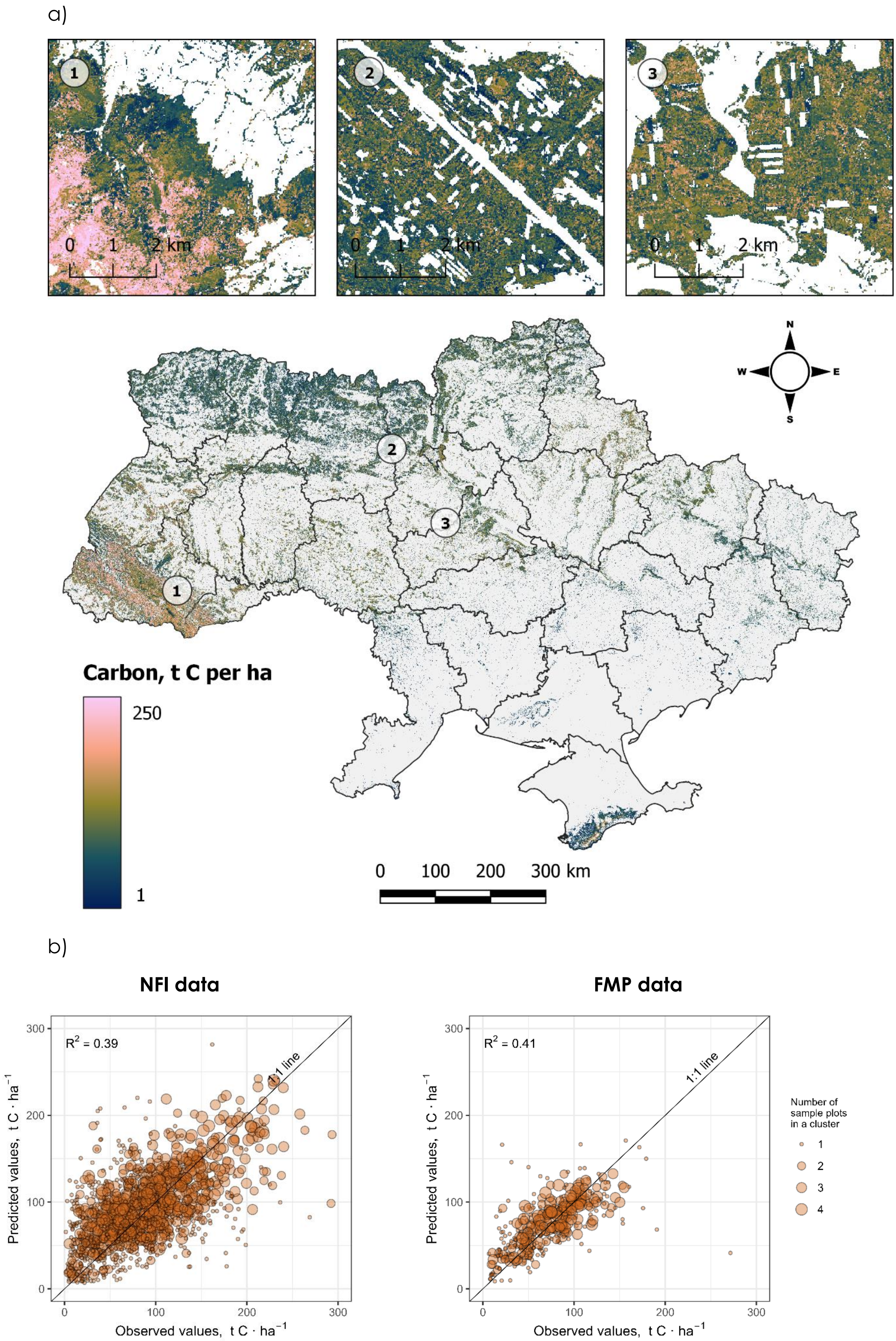

Figure 14. Carbon stock in LB (2023): a) map predicted using the GNN imputation model, b) observed versus predicted values.

3.4. Uncertainties of the estimates

Uncertainties in map area estimates were accounted for using confusion matrices. We used a stratified sampling following the recommendations by Olofsson et al. (2014). Given the varying ability of the RF classification models to account for commission and omission errors, the actual area of map classes may differ from that calculated from the map. Therefore, we provide also adjusted values and 95% SE of the area estimates (eq. 8–11).

Uncertainties of continuous forest attributes were calculated using the MAR estimation procedure (McConville et al., 2020). Similarly, the GREG estimator (eq. 12–14) was used to obtain adjustments and SE of forest attributes. We presented MAR estimates for mean and total values of attributes at the level of Ukraine (Table 10 and Table 11), Gensiruk's ecozones, and for areas affected (unaffected) during the war. Results at the regional level are provided in a supplementary file and include estimates of forest area and forest attributes structured by 1) SRTM elevation and slope intervals; 2) 20-year age intervals; 3) 50-m^3 GSV intervals; 4) 20-cm DBH classes; 5) 5-m HT classes.

3.5. Limitations of the RS-Inventory

This study represents the first implementation of a remote sensing-based assessment of Ukrainian forests. Examples from countries that have pioneered this approach (e.g. USA, Finland) show that there is a constant need to balance technological advances, research, and operational needs. In this regard, some current limitations of the RS inventory can be identified.

1. The project demonstrated an approach capable of producing wall-to-wall forest maps in Ukraine. The main limitation of the approach is that the developed maps include all tree vegetation, including urban forests, trees in residential areas, cemeteries, etc. This information does not directly address the problem of assessing the State Forest Fund, but can shed light on many other important issues, including the identification of forest regrowth areas outside the forest. The actual forest area can be assessed within the boundaries of forest stands.
2. Sentinel TS showed good performance in mapping forests in Ukraine. However, there are still problems with mapping narrow shelterbelts.
3. Accuracy of mapped attributes can be properly addressed when sufficient field observations are available for small areas of interest. The lack of field data for many regions in Ukraine has not allowed us to make statistically sound estimates. However, there is good potential to address this issue as new observations are collected.
4. Optical satellite TS have limitations in terms of signal saturation for dense and multilayered forest stands. Therefore, integrations of active remote sensing capable of penetrating dense canopies seem very promising for more accurate classification of tree species and mapping of forest attributes.

Table 10. The RS-Inventory estimates of forested area and mean values of forest attributes in Ukraine for 2023.

Groups2	Estimate	Area (ha)	Age (years)	DBH (cm)	HT (m)	BA ($m^2 \cdot ha^{-1}$)	GSV ($m^3 \cdot ha^{-1}$)	Density ($n \cdot ha^{-1}$)	LB ($t \cdot ha^{-1}$)	Carbon ($t \cdot ha^{-1}$)	CO_2-equiv. ($t \cdot ha^{-1}$)
All species	Map-based values	11335437	59.1	28.3	20.5	25.5	263.5	506.4	188.0	88.3	323.9
All species	Adjusted values	11209004	57.1	27.6	19.9	24.8	251.0	549.6	179.3	84.3	308.9
All species	*95% SE of adjusted values*	*166099*	*0.9*	*0.4*	*0.2*	*0.4*	*4.9*	*36.9*	*3.7*	*1.8*	*6.4*
All coniferous	Map-based values	3768364	59.5	29.1	21.2	29.5	313.9	583.9	183.1	86.0	315.5
All coniferous	Adjusted values	3835955	57.5	28.8	20.7	28.7	299.4	614.4	168.3	79.1	290.0
All coniferous	*95% SE of adjusted values*	*86580*	*1.4*	*0.6*	*0.4*	*0.6*	*8.9*	*54.5*	*5.3*	*2.5*	*9.1*
All deciduous	Map-based values	7567072	59.0	27.9	20.1	23.5	238.4	467.7	190.4	89.5	328.1
All deciduous	Adjusted values	7373048	56.8	27.0	19.5	22.7	225.9	515.8	185.0	86.9	318.7
All deciduous	*95% SE of adjusted values*	*86580*	*1.1*	*0.5*	*0.3*	*0.4*	*5.8*	*49.1*	*5.1*	*2.4*	*8.8*
Pine	Map-based values	3049782	57.6	28.5	20.7	27.6	287.2	588.1	167.1	78.5	288.0
Pine	Adjusted values	3109940	56.2	28.3	20.3	26.9	274.6	605.2	155.7	73.2	268.2
Pine	*95% SE of adjusted values*	*92643*	*1.5*	*0.6*	*0.5*	*0.7*	*9.4*	*60.6*	*5.8*	*2.7*	*9.9*
Spruce (Fir)	Map-based values	718582	67.2	31.8	23.1	38.0	427.5	566.1	250.7	117.8	432.0
Spruce (Fir)	Adjusted values	726016	63.3	30.7	22.2	36.8	405.7	654.1	222.4	104.5	383.3
Spruce (Fir)	*95% SE of adjusted values*	*43615*	*3.2*	*1.2*	*0.8*	*1.5*	*21.5*	*119.3*	*12.0*	*5.6*	*20.7*
Oak	Map-based values	1478065	65.6	29.9	21.2	23.8	250.5	398.4	204.1	95.9	351.8
Oak	Adjusted values	1644950	73.9	32.9	21.9	24.3	263.3	249.1	224.0	105.3	386.0
Oak	*95% SE of adjusted values*	*114163*	*2.3*	*1.0*	*0.5*	*0.8*	*10.2*	*55.1*	*9.0*	*4.2*	*15.5*
Beech	Map-based values	951818	68.0	32.5	22.8	31.7	349.2	443.9	309.5	145.5	533.4
Beech	Adjusted values	773897	74.2	35.7	24.7	32.8	369.7	260.4	353.6	166.2	609.3
Beech	*95% SE of adjusted values*	*60755*	*3.4*	*1.5*	*1.0*	*1.6*	*22.6*	*120.8*	*21.3*	*10.0*	*36.7*
Ash, Linden, Maple, Black locust	Map-based values	2406848	58.5	26.1	18.2	21.3	200.6	498.9	160.0	75.2	275.8
Ash, Linden, Maple, Black locust	Adjusted values	2217394	52.6	23.5	17.0	20.4	185.3	653.5	152.9	71.9	263.6
Ash, Linden, Maple, Black locust	*95% SE of adjusted values*	*110993*	*2.1*	*1.0*	*0.5*	*0.8*	*9.3*	*100.6*	*8.6*	*4.1*	*14.9*
Birch, Alder, Poplar	Map-based values	2398709	52.1	26.5	19.9	22.0	219.7	489.8	158.9	74.7	273.8
Birch, Alder, Poplar	Adjusted values	2223998	43.5	23.8	18.5	19.9	185.2	654.5	121.7	57.2	209.8
Birch, Alder, Poplar	*95% SE of adjusted values*	*133157*	*2.1*	*1.1*	*0.6*	*0.9*	*11.9*	*127.3*	*8.8*	*4.2*	*15.2*
Hornbeam	Map-based values	331632	57.1	28.9	21.9	26.3	277.5	459.5	235.7	110.8	406.1
Hornbeam	Adjusted values	512809	52.0	23.9	18.9	24.8	240.5	560.0	218.0	102.5	375.6
Hornbeam	*95% SE of adjusted values*	*72702*	*3.5*	*1.9*	*1.2*	*1.6*	*20.6*	*127.7*	*19.4*	*9.1*	*33.4*

Table 11. The RS-Inventory estimates of forested area and total values of forest attributes in Ukraine for 2023.

Groups2	Estimate	Area (ha)	GSV (mln m³)	Density (mln)	LB (mln t)	Carbon (mln t)	CO_2-equiv. (mln t)
All species	Map-based values	11335437	2987.30	5739.83	2130.62	1001.39	3671.77
All species	Adjusted values	11209004	2813.76	6159.93	2009.22	944.38	3462.46
All species	*95% SE of adjusted values*	*166099*	*54.92*	*413.61*	*41.47*	*20.18*	*71.74*
All coniferous	Map-based values	3768364	1182.99	2200.49	689.80	324.21	1188.76
All coniferous	Adjusted values	3835955	1148.47	2356.97	645.53	303.42	1112.42
All coniferous	*95% SE of adjusted values*	*86580*	*34.14*	*209.06*	*20.33*	*9.59*	*34.91*
All deciduous	Map-based values	7567072	1804.31	3539.35	1440.82	677.18	2483.01
All deciduous	Adjusted values	7373048	1665.29	3802.96	1363.69	640.96	2350.04
All deciduous	*95% SE of adjusted values*	*86580*	*42.76*	*362.02*	*37.60*	*17.70*	*64.88*
Pine	Map-based values	3049782	875.80	1793.67	509.68	239.55	878.34
Pine	Adjusted values	3109940	853.89	1882.08	484.06	227.52	834.16
Pine	*95% SE of adjusted values*	*92643*	*29.23*	*188.46*	*18.04*	*8.40*	*30.79*
Spruce (Fir)	Map-based values	718582	307.19	406.82	180.13	84.66	310.42
Spruce (Fir)	Adjusted values	726016	294.58	474.89	161.47	75.90	278.26
Spruce (Fir)	*95% SE of adjusted values*	*43615*	*15.61*	*86.61*	*8.71*	*4.07*	*15.03*
Oak	Map-based values	1478065	370.24	588.87	301.71	141.80	519.95
Oak	Adjusted values	1644950	433.14	409.75	368.43	173.17	634.89
Oak	*95% SE of adjusted values*	*114163*	*16.78*	*90.64*	*14.80*	*6.91*	*25.50*
Beech	Map-based values	951818	332.35	422.47	294.59	138.46	507.68
Beech	Adjusted values	773897	286.12	201.50	273.65	128.62	471.57
Beech	*95% SE of adjusted values*	*60755*	*17.49*	*93.49*	*16.48*	*7.74*	*28.40*
Ash, Linden, Maple, Black locust	Map-based values	2406848	482.73	1200.74	385.21	181.05	663.85
Ash, Linden, Maple, Black locust	Adjusted values	2217394	410.83	1449.03	339.12	159.39	584.43
Ash, Linden, Maple, Black locust	*95% SE of adjusted values*	*110993*	*20.62*	*223.07*	*19.07*	*9.09*	*33.04*
Birch, Alder, Poplar	Map-based values	2398709	526.97	1174.86	381.15	179.14	656.84
Birch, Alder, Poplar	Adjusted values	2223998	411.87	1455.53	270.72	127.24	466.54
Birch, Alder, Poplar	*95% SE of adjusted values*	*133157*	*26.47*	*283.12*	*19.57*	*9.34*	*33.80*
Hornbeam	Map-based values	331632	92.02	152.40	78.15	36.73	134.68
Hornbeam	Adjusted values	512809	123.34	287.16	111.77	52.54	192.62
Hornbeam	95% SE of adjusted values	72702	10.56	65.49	9.95	4.67	17.13

CONCLUSION AND FUTURE PROSPECTS

The methodology of the RS-Inventory is based on the latest advances in data processing using terrestrial and remotely sensed observations. The project integrates international expertise in many fields including field data collection, statistical assessment, satellite data processing, modeling, etc. In addition to the traditional design-based NFI, the proposed approach provides a basis for both forest mapping and forest assessment across Ukraine including territories that are not available for field visits. From this perspective, we combined multiyear sample plots of the NFI with the most recent FMP data to obtain complete coverage of Ukraine with reference data. Given the multiyear reference information, we used the time series of Sentinel 2 time series for mapping and statistical evaluation of the NFI attributes. The following conclusions can be drawn from this report.

TECHNICHAL ASPECTS

Processing timeline. The RS-Inventory relies on two main sources of information: 1) NFI sample plots, and 2) satellite time series. While the processing of sample plot data can start once the last plot in the current year has been sampled, the processing of satellite data must start on January 1 of the year following the field season. This is important in order to have a complete TS for the whole year.

Earth observation data. Time series of free Sentinel 2 observations can be a standard choice for further implementation of the RS-Inventory of Ukraine given the free access to satellite imagery, high data quality, and detailed spectral resolution of 20 m. Given multiyear NFI observations, the application of satellite time series is crucial for their complex use in new phases of forest inventory. In this way, each new assessment will be more precise as it will use more field observations. This is also an important point for the use of historical FMP data.

Data processing platform. Given the large volume of information, there is a need for cloud-based computing to accelerate many steps of the analysis of remote sensing data. For this reason, we used the GEE platform which offers free access only to the computing facilities for research and academic use with a fixed quota. In the case of operational use of the platform, commercial accounts with an adjusted quota plan may also be an option.

Quality of sample plot data. There are several important aspects of data quality. First, the coordinates of plot centers must be obtained with the highest accuracy. This is critical to ensure that plots and pixels match exactly. Second, the RS-Inventory only works with plots that are fully (or at least >75%) forested and sampled within the same stand. Visual inspection of each sample plot using high resolution imagery is required for the next steps of the RS-Inventory to improve the quality of the output maps and tables.

METHODOLOGICAL ASPECTS

Mapping species composition. This study reports mainly on area and estimates for groups of dominant species which provided reasonable accuracy. However, individual species can be mapped with further improvements in the methodology. In particular, more efforts are needed to understand the spatial boundaries of ecological niches of species (i.e., combinations of environmental variables).

Carbon stock assessment. The carbon stock of LB was estimated using stand-level models. For the future application, carbon stock estimation needs to be integrated into plot-level processing workflow using tree-level models similar to GSV.

SUGGESTIONS FOR THE FUTURE DEVELOPMENT OF THE METHODOLOGY

Forest area compliant with national definition of forests. The result of the RS-Inventory provides the basis for a national-wide estimation of forested area once the assessment is carried out within the officially recognized boundaries of the State Forest Fund of Ukraine.

Prospects for continuous forest monitoring. The RS-Inventory can be used for periodic (annual) updating forest maps (FNF, forest attributes) in Ukraine. In addition to wall-to-wall maps, the approach can be used to identify forest disturbances, including logging, thinning, wildfires, insects, and other types of change agents.

Implications for FMP and timber industry. While RS-Inventory provides pixel-based outputs, the FMP still requires polygon-based forest information. Therefore, the distribution of forest area or attributes by species, age classes, etc. need to be obtained using aggregated pixel data at the stand level. Addressing this issue is important to support the officially recognized methodology in Ukraine for planning the allowable annual cut. Nevertheless, the developed pixel maps and potentially available data on disturbed forests have direct implications for forest management planning and salvage logging in war-damaged areas that are not yet accessible for field surveys.

Assessing forests over small areas of interests. The maps can be used for small area assessment (SAE) of forests on a smaller scale than the national level. This was demonstrated using examples of Gensiruk's ecozones and war-affected areas. The accuracy of SAE can vary in terms of variance and bias at the level of region(s), protected areas, ownership or use rights. Therefore, model-assisted estimation techniques must be used to obtain accurate estimates. This is highly dependent on the available sample plot observations collected within the area of interest and may not be feasible for very small areas. For maps, one would expect more variability in predicted values at the pixel level. The study showed that the agreement between observed and predicted values is better for multi-pixel blocks than for individual pixels (i.e. R-squared values are higher when assessed at cluster level). This provides an opportunity for map users to choose the appropriate level of aggregation to obtain a more reliable spatial pattern, albeit at a coarser resolution.

TABLES

FIGURES

ANNEXES

ANNEX 1. LAND COVER ATLAS USED IN PHOTOINTEPRETATION

1. Forest

1.1. Shelterbelt

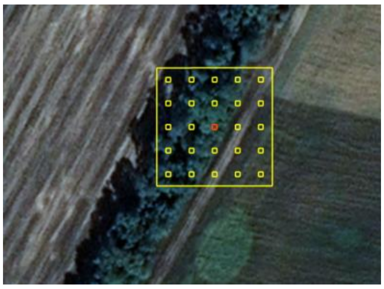

1.2. Forest Regrowth

1.3. Urban Forest

1.4. Other forest

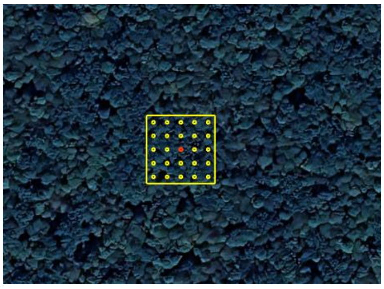

2. Other woody vegetation

2.1. Forest Edge

2.2. Damaged Forest

2.3. Shrubland

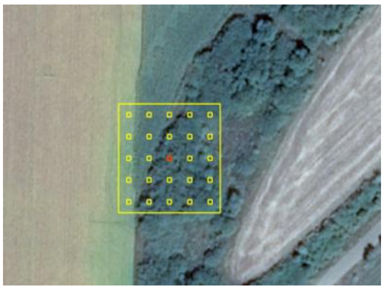

2.4. Orchard

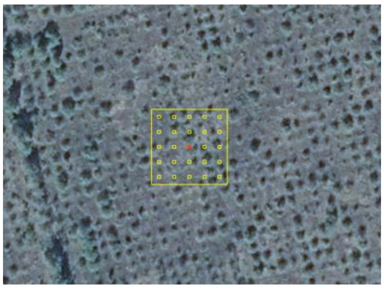

2.5. Garden Trees

2.6 OWV

3. Grassland

3.1. Meadow

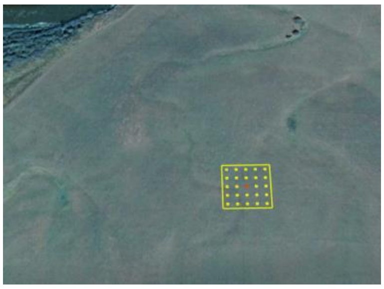

3.2. Barren

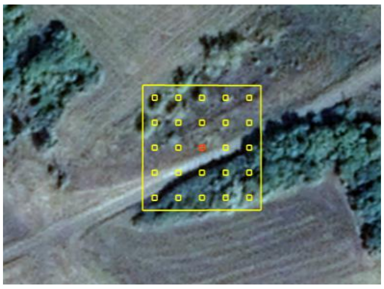

3.3. Glade

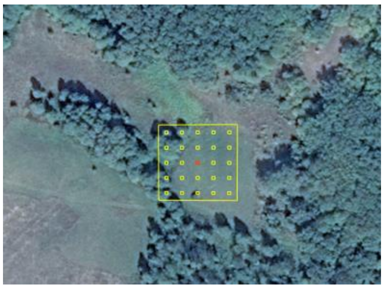

3.4 Other grassland

4. Cropland

4.1. Fallow Cropland

4.2. Irrigated Cropland

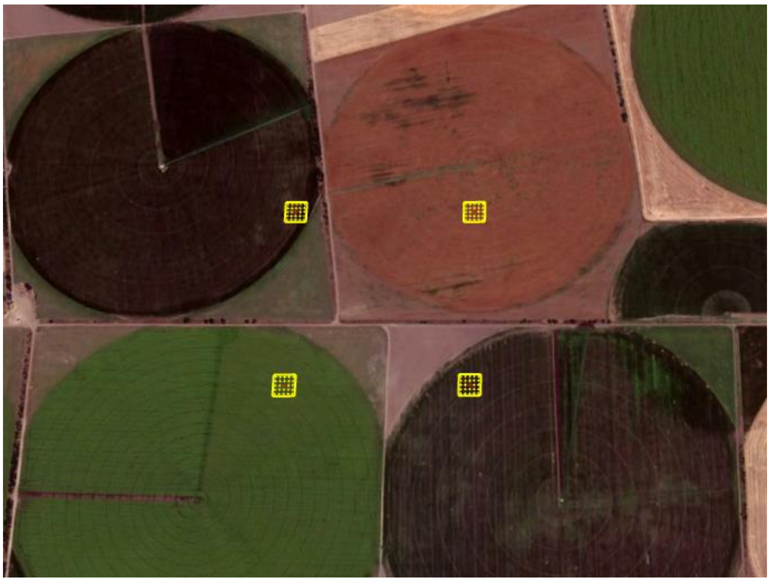

4.3. Other cropland

5. Wetland

5.1. Seasonal water

5.2. Peatland

5.3. Riparian vegetation

6. Water

6.1. Permanent river

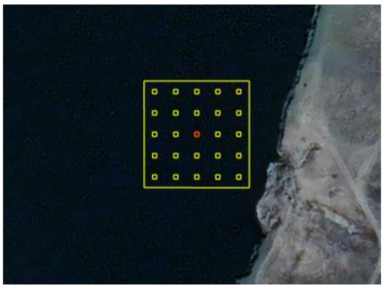

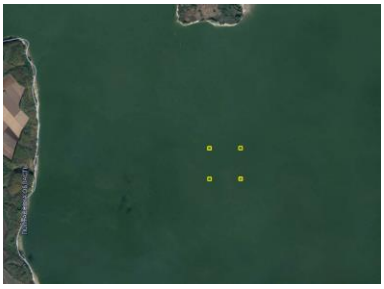

6.2. Permanent Lake

6.3 Sea

7. Urban (unproductive)

7.1. Highway

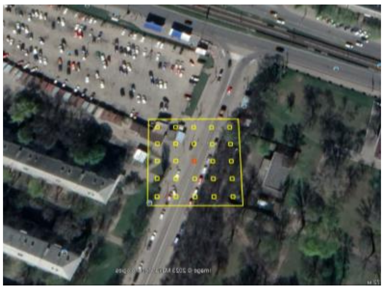

7.2. Building

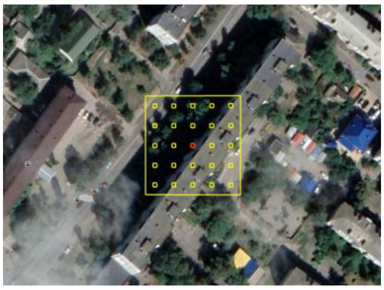

7.5. Other unproductive

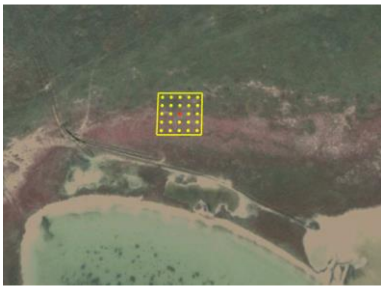

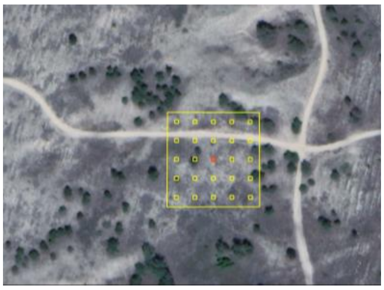

REFERENCES

Abatzoglou, J. T., Dobrowski, S. Z., Parks, S. A., & Hegewisch, K. C. (2018). TerraClimate, a high-resolution global dataset of monthly climate and climatic water balance from 1958–2015. *Scientific Data*, *5*(1), 170191. https://doi.org/10.1038/sdata.2017.191

Bey, A., Sánchez-Paus Díaz, A., Maniatis, D., Marchi, G., Mollicone, D., Ricci, S., Bastin, J.-F., Moore, R., Federici, S., Rezende, M., Patriarca, C., Turia, R., Gamoga, G., Abe, H., Kaidong, E., & Miceli, G. (2016). Collect Earth: Land Use and Land Cover Assessment through Augmented Visual Interpretation. *Remote Sensing*, *8*(10), 807. https://doi.org/10.3390/rs8100807

Bilous, A. M., Kashpor, S. M., Myroniuk, V. V., Svynchyk, V. A., & Lesnik, O. M. (Eds.). (2020). *Forest Inventory Handbook*. Dnipro: Lira LTD, 2020, 364 [in Ukrainian].

Breiman, L. (2001). Random forests. *Machine Learning*, *45*(1), 5–32. https://doi.org/10.1023/a:1010933404324

Gensiruk, S. A. (1992). *Forests of Ukraine*. Kyiv: Naukova dumka (in Ukrainian).

Gorelick, N., Hancher, M., Dixon, M., Ilyushchenko, S., Thau, D., & Moore, R. (2017). Google Earth Engine: Planetary-scale geospatial analysis for everyone. *Remote Sensing of Environment*, *202*, 18–27. https://doi.org/10.1016/j.rse.2017.06.031

Kershaw, J. A., Ducey, M. J., Beers, T., & Hush, B. (2016). *Forest Mensuration, 5th ed*.

McConville, K. S., Moisen, G. G., & Frescino, T. S. (2020). A Tutorial on Model-Assisted Estimation with Application to Forest Inventory. *Forests*, *11*(2), 244. https://doi.org/10.3390/f11020244

McRoberts, R. E., Liknes, G. C., & Domke, G. M. (2014). Using a remote sensing-based, percent tree cover map to enhance forest inventory estimation. *Forest Ecology and Management*, *331*, 12–18. https://doi.org/10.1016/j.foreco.2014.07.025

McRoberts, R. E., Vibrans, A. C., Sannier, C., Næsset, E., Hansen, M. C., Walters, B. F., & Lingner, D. V. (2016). Methods for evaluating the utilities of local and global maps for increasing the precision of estimates of subtropical forest area. *Canadian Journal of Forest Research*, *46*(7), 924–932. https://doi.org/10.1139/cjfr-2016-0064

Myroniuk, V. (2023). *Remote Sensing Based Forest Inventory of Ukraine (RS-Inventory): Case Study for Sumy Administrative Oblast*.

Myroniuk, V., Bell, D. M., Gregory, M. J., Vasylyshyn, R., & Bilous, A. (2022). Uncovering forest dynamics using historical forest inventory data and Landsat time series. *Forest Ecology and Management*, *513*, 120184. https://doi.org/10.1016/j.foreco.2022.120184

Ohmann, J. L., & Gregory, M. J. (2002). Predictive mapping of forest composition and structure with direct gradient analysis and nearest- neighbor imputation in coastal Oregon, U.S.A. *Canadian Journal of Forest Research*, *32*(4), 725–741. https://doi.org/10.1139/x02-011

Olofsson, P., Foody, G. M., Herold, M., Stehman, S. V., Woodcock, C. E., & Wulder, M. A. (2014). Good practices for estimating area and assessing accuracy of land change. *Remote Sensing of Environment*, *148*, 42–57. https://doi.org/10.1016/j.rse.2014.02.015

Shvidenko, A. Z., Lakyda, P. I., Schepaschenko, D. G., Vasylyshyn, R. D., & Marchuk, Yu. M. (2014). *Carbon, climate and land-use in Ukraine: Forest sector*. IE V.M. Gavryshenko.

Weinreich, A., Sperlich, M., Myroniuk, V., & Farion, Y. (2023). *Concept Study: Remote Sensing Based National Forest Inventory Support* (W-UKR 21-01; p. 62). unique land use GmbH. https://www.sfi-ukraine.org.ua/wp-content/uploads/2023/10/2023-03-31-concept-study-rs-support-for-nfi-ukraine.pdf

Weiss, A. (2001). *Topographic Position and Landforms Analysis.* [Poster presentation]. ESRI User Conference, San Diego, CA.

Zhu, Z., & Woodcock, C. E. (2014). Continuous change detection and classification of land cover using all available Landsat data. *Remote Sensing of Environment*, *144*, 152–171. https://doi.org/10.1016/j.rse.2014.01.011